Journal of Computational Mathematics
Vol.42, No.1, 2024, 217–247.

http://www.global-sci.org/jcm
doi:10.4208/jcm.2203-m2021-0244

LEGENDRE-GAUSS-RADAU SPECTRAL COLLOCATION METHOD FOR NONLINEAR SECOND-ORDER INITIAL VALUE PROBLEMS WITH APPLICATIONS TO WAVE EQUATIONS*

Lina Wang
Department of Mathematics, Shanghai Normal University, Shanghai 200234, China;
School of Science, Henan University of Engineering, Zhengzhou 451191, China
Email: 1000481187@smail.shnu.edu.cn
Qian Tong, Lijun Yi[1)] and Mingzhu Zhang
Department of Mathematics, Shanghai Normal University, Shanghai 200234, China
Email: 944827476@qq.com, ylj5152@shnu.edu.cn, niruochenxi@163.com

Abstract

We propose and analyze a single-interval Legendre-Gauss-Radau (LGR) spectral collocation method for nonlinear second-order initial value problems of ordinary differential equations. We design an efficient iterative algorithm and prove spectral convergence for the single-interval LGR collocation method. For more effective implementation, we propose a multi-interval LGR spectral collocation scheme, which provides us great flexibility with respect to the local time steps and local approximation degrees. Moreover, we combine the multi-interval LGR collocation method in time with the Legendre-Gauss-Lobatto collocation method in space to obtain a space-time spectral collocation approximation for nonlinear second-order evolution equations. Numerical results show that the proposed methods have high accuracy and excellent long-time stability. Numerical comparison between our methods and several commonly used methods are also provided.

Mathematics subject classification: 65M70, 41A10, 65L05, 35L05.
Key words: Legendre-Gauss-Radau collocation method, Second-order initial value problem, Spectral convergence, Wave equation.

1. Introduction

The initial value problems (IVPs) of second-order ordinary differential equations (ODEs) appear in many fields of science and engineering. In addition, a large number of second-order evolution equations, especially nonlinear wave equations, such as the Klein-Gordon and sine-Gordon equations, are often transformed into IVPs of second-order ODEs after appropriate spatial discretization methods. In the past few decades, great progress has been made in the study of numerical methods for the IVPs of (second-order) ODEs. Traditional and frequently used approaches for the numerical integration of (second-order) ODEs are mainly based on implicit and explicit finite difference, Runge-Kutta and Newmark-type schemes. We refer the reader to the monographs [8, 25, 26, 28, 29, 36, 41] for a comprehensive review.

As we all know, spectral methods have become important numerical methods for solving partial differential equations (PDEs), and have a wide range of applications in many fields of scientific and engineering computation, see, e.g., [6, 7, 10, 16, 18, 19, 40] and the references

* Received August 24, 2021 / Revised version received November 23, 2021 / Accepted March 28, 2022 / Published online February 21, 2023 /
1) Corresponding author

therein. Due to their high accuracy, spectral methods (including spectral collocation methods) have been applied to the numerical integration of ODEs in recent years. For example, Guo *et al.* developed several Laguerre spectral collocation methods [20, 23, 51, 52] and Legendre spectral collocation methods [21, 22, 24, 47] for nonlinear first and second-order IVPs of ODEs. In [1, 2], several spectral Galerkin and collocation methods were introduced for the numerical solutions of nonlinear Hamiltonian (ODE) systems. For some other high order methods (including the *hp*-version continuous and discontinuous Galerkin methods) for IVPs of ODEs, we refer the reader to [3, 39, 48, 49, 53] and the references therein.

The main purpose of the present paper is to introduce and analyze a new spectral collocation method based on Legendre-Gauss-Radau (LGR) points for the second-order ODEs of the form

$$\begin{cases} u''(t) = f(u'(t), u(t), t), & t \in (0, T], \\ u'(0) = v_0, & u(0) = u_0, \end{cases} \tag{1.1}$$

where the values v_0 and u_0 describe the initial states of $u(t)$ and f is a given function. For ease of statement, we sometimes use the notations $\partial_t u$ and $\partial_t^2 u$ instead of u' and u'', respectively.

We first design a single-interval spectral collocation scheme for problem (1.1) based on $N+1$ LGR points (see (2.21)). We then construct a simple but efficient iterative algorithm for numerical implementation of the single-interval collocation scheme by using Legendre polynomial expansion. We carry out a rigorous error analysis for the proposed scheme. Theoretical results show that the single-interval LGR collocation scheme has spectral accuracy, namely, for any fixed mode N, the smoother the exact solution is, the more accurate the numerical solution is. We also note that a Legendre-Gauss (LG) spectral collocation method has been proposed and analyzed in [24] for second-order ODEs. The main differences between the present paper and [24] are as follows: 1) Our collocation scheme is based on the LGR points, while the scheme in [24] is based on the LG points, this brings us different considerations in the theoretical analysis; 2) Due to different choices of the collocation points and different analysis approaches, the convergence of our method in N is half order higher than the method developed in [24] (see also Remark 2.2); 3) We design a new fixed-point iterative algorithm, which is much simpler and faster than that in [24] (see numerical comparison in subsection 2.5.2).

In order to improve the computational efficiency, we further propose a multi-interval LGR collocation method based on domain decomposition. Roughly speaking, we divide the solution interval $(0, T]$ into a series of non-overlapping subintervals, and then adopt the single-interval LGR collocation scheme and the corresponding iterative algorithm to obtain local approximation on each subinterval. The multi-interval LGR collocation scheme has the following advantages:

- For large T, we can obtain the numerical solution by the single-interval LGR collocation method on each subinterval step by step. In particular, the corresponding nonlinear algebraic system on each subinterval usually contains only a small number of unknowns. Therefore, the multi-interval collocation scheme can be implemented efficiently and economically. At the same time, it keeps the global spectral accuracy.
- The multi-interval LGR collocation scheme has great flexibility with respect to the local time steps and local approximation degrees. It is a variable-step and variable-order scheme. This feature makes it easy for us to deal with solutions with complex dynamic behaviors, such as oscillatory, singular and long-time behaviors.

- We use the LGR points (with right endpoint) instead of LG points as collocation points, and thus we can obtain the initial values of the local problem to be solved on the current subinterval from the computed results on the previous subinterval directly. This feature simplifies actual calculations and saves some works.

- The multi-interval LGR collocation scheme produces global numerical solutions, which can provide more information about the structures of the exact solutions. However, the usual difference methods do not have such merit.

As an application, we apply the multi-interval LGR method to the time discretization of nonlinear second-order evolution equations. More specifically, we combine the Legendre-Gauss-Lobatto (LGL) collocation method in space with the multi-interval LGR method in time to obtain a fully discrete space-time spectral collocation approximation. We also take two typical nonlinear wave equations, such as Klein-Gorden and sine-Gorden equations as examples. Numerical results show that the proposed space-time collocation scheme has excellent long-time stability and spectral accuracy in both space and time. By the way, it is worth mentioning that such space-time high order methods for time dependent PDEs have received considerable attention in recent years, see, e.g., the space-time spectral Galerkin and collocation methods [30, 31, 35, 42–45, 54, 55, 57, 58], the space-time hp-finite element methods [4, 5, 9, 13, 32, 38] and the references therein. We would like to emphasize that our purpose is not to compare with those existing space-time high order methods, but to develop a new and available space-time collocation method for nonlinear second-order evolution equations.

The paper is organized as follows. In Section 2, we introduce and analyze a single-interval LGR collocation method for nonlinear second-order IVPs of ODEs. We further propose a multi-interval LGR collocation method for more effective implementation. We also provide some numerical examples and comparison to show the high accuracy and efficiency of the single and multi-interval LGR collocation methods. In Section 3, we design a space-time spectral collocation scheme for the nonlinear second-order evolution equations based on the multi-interval LGR collocation method in time and the LGL collocation method in space. We take two typical nonlinear wave equations as examples, numerical results show that the space-time collocation scheme has long-time stability and high accuracy in both space and time. Finally, we give some concluding remarks in Section 4.

2. Legendre-Gauss-Radau Spectral Collocation Method for Second-Order IVPs

In this section, we introduce and analyze a single-interval LGR collocation method for the model problem (1.1).

2.1. Preliminaries

Let $L_l(x)$ be the Legendre polynomial of degree l on $\Lambda := [-1, 1]$. The Legendre polynomials satisfy the recursion relation

$$(l+1)L_{l+1}(x) = (2l+1)xL_l(x) - lL_{l-1}(x), \quad l \geq 1, \tag{2.1}$$

where $L_0(x) = 1$ and $L_1(x) = x$. We recall that the Legendre polynomials also satisfy the orthogonality relation

$$\int_{-1}^{1} L_l(x)L_m(x)dx = \frac{2}{2l+1}\delta_{lm}, \quad \forall\, n, m \geq 0. \tag{2.2}$$

For any $u, v \in L^2(\Lambda)$, we denote by $(\cdot,\cdot)$ the inner product and by $\|\cdot\|$ the L^2-norm of the space $L^2(\Lambda)$, i.e.,

$$(u, v) = \int_{\Lambda} uvdx, \quad \|v\| = (v, v)^{\frac{1}{2}}. \tag{2.3}$$

Let $\{x_j^N\}_{j=0}^N$ be the set of LGR quadrature nodes (arranged in ascending order with fixed right endpoint $x_N^N = 1$) and $\{\omega_j^N\}_{j=0}^N$ be the corresponding weights. We recall that $\{x_j^N\}_{j=0}^N$ are the distinct zeros of $L_{N+1}(x) - L_N(x), x \in \Lambda$. For any $u, v \in L^2(\Lambda)$, we define the discrete inner product $(\cdot,\cdot)_N$ and the discrete norm $\|\cdot\|_N$ by

$$(u, v)_N = \sum_{j=0}^{N} u(x_j^N)v(x_j^N)\omega_j^N, \quad \|v\|_N = (v, v)_N^{\frac{1}{2}}.$$

Let $\mathcal{P}_N(\Lambda)$ be the set of polynomials of degree at most N. Due to the exactness of the LGR quadrature (cf. [40]), for any $\phi\psi \in \mathcal{P}_{2N}(\Lambda)$ and $\varphi \in \mathcal{P}_N(\Lambda)$, there hold

$$(\phi, \psi) = (\phi, \psi)_N, \quad \|\varphi\| = \|\varphi\|_N. \tag{2.4}$$

In addition, for any $v \in C(-1, 1]$, we define the standard LGR interpolation $\mathcal{I}_N v \in \mathcal{P}_N(\Lambda)$ by

$$\mathcal{I}_N v(x_j^N) = v(x_j^N), \quad 0 \leq j \leq N.$$

For our purpose, we now define the shifted Legendre polynomials $L_{T,l}(t)$ by

$$L_{T,l}(t) = L_l\left(\frac{2t}{T} - 1\right), \quad t \in [0, T], \quad l \geq 0.$$

Due to (2.1), the shifted Legendre polynomials also satisfy the recursion relation

$$(l+1)L_{T,l+1}(t) = (2l+1)\left(\frac{2t}{T} - 1\right)L_{T,l}(t) - lL_{T,l-1}(t), \quad l \geq 1. \tag{2.5}$$

By (2.2), there holds

$$\int_0^T L_{T,l}(t)L_{T,m}(t)dt = \frac{T}{2l+1}\delta_{lm}, \tag{2.6}$$

which implies that the set of $\{L_{T,l}(t), l \geq 0\}$ forms a complete $L^2(0, T)$-orthogonal system. Hence, for any $v \in L^2(0, T)$, we have

$$v(t) = \sum_{l=0}^{\infty} \hat{v}_l L_{T,l}(t) \quad \text{with} \quad \widehat{v}_l = \frac{2l+1}{T}\int_0^T v(t)L_{T,l}(t)dt. \tag{2.7}$$

Similar to (2.3), we denote by $(\cdot,\cdot)_T$ the continuous inner product and by $\|\cdot\|_T$ the L^2-norm of the space $L^2(0, T)$. Clearly, we have $\|v\|_T = (v, v)_T^{\frac{1}{2}}$ for any $v \in L^2(0, T)$.

Furthermore, we define the shifted LGR nodes and weights $\{t_{T,j}^N, \omega_{T,j}^N\}_{j=0}^N$ by

$$t_{T,j}^N = \frac{T}{2}(x_j^N + 1), \quad \omega_{T,j}^N = \frac{T}{2}\omega_j^N, \quad 0 \leq j \leq N.$$

Analogously, for any $u, v \in L^2(0,T)$, we define the discrete inner product $(\cdot,\cdot)_{T,N}$ and norm $\|\cdot\|_{T,N}$ by

$$(u,v)_{T,N} = \sum_{j=0}^{N} \omega_{T,j}^N u(t_{T,j}^N) v(t_{T,j}^N), \quad \|v\|_{T,N} = (v,v)_{T,N}^{\frac{1}{2}}.$$

Thanks to (2.4), for any $\phi\psi \in \mathcal{P}_{2N}(0,T)$ and $\varphi \in \mathcal{P}_N(0,T)$, there hold

$$(\phi,\psi)_T = (\phi,\psi)_{T,N}, \quad \|\varphi\|_T = \|\varphi\|_{T,N}. \tag{2.8}$$

For any $v \in C(0,T]$, we then define the shifted LGR interpolation $\mathcal{I}_{T,N}v \in \mathcal{P}_N(0,T)$ by

$$\mathcal{I}_{T,N}v(t_{T,j}^N) = v(t_{T,j}^N), \quad 0 \le j \le N. \tag{2.9}$$

From (2.8), we find that

$$(\mathcal{I}_{T,N}v, \phi)_T = (\mathcal{I}_{T,N}v, \phi)_{T,N} = (v,\phi)_{T,N}, \quad \forall \phi \in \mathcal{P}_N(0,T). \tag{2.10}$$

Obviously, the shifted LGR interpolation $\mathcal{I}_{T,N}v$ can be expanded as

$$\mathcal{I}_{T,N}v(t) = \sum_{l=0}^{N} \widetilde{v}_l L_{T,l}(t) \tag{2.11}$$

with

$$\widetilde{v}_l = \frac{2l+1}{T}(\mathcal{I}_{T,N}v, L_{T,l})_T = \frac{2l+1}{T}(v, L_{T,l})_{T,N}, \quad 0 \le l \le N. \tag{2.12}$$

For any nonnegative integer r, let $H^r(0,T)$ be the usual Sobolev space. For simplicity, we also denote by $\|\cdot\|_{r,T}$ and $|\cdot|_{r,T}$ the norm and semi-norm of the space $H^r(0,T)$, respectively. In particular, we set $\|\cdot\|_{0,T} = \|\cdot\|_T$ for $r=0$.

In view of (5.4.33) and (5.4.34) of [10], for any $u \in H^r(\Lambda)$ with integer $1 \le r \le N+1$ and $1 \le m \le r$, there hold

$$\|u - \mathcal{I}_N u\|_{L^2(\Lambda)} \le CN^{-r}|u|_{H^r(\Lambda)},$$
$$|u - \mathcal{I}_N u|_{H^m(\Lambda)} \le CN^{2m-\frac{1}{2}-r}|u|_{H^r(\Lambda)}$$

for the standard LGR interpolation $\mathcal{I}_N u$. Then, we can easily obtain the following scaled estimates for the shifted LGR interpolation.

Lemma 2.1. *Let $u \in H^r(0,T)$ with integer $1 \le r \le N+1$. For $1 \le m \le r$, there hold*

$$\|u - \mathcal{I}_{T,N}u\|_T \le CT^r N^{-r}|u|_{r,T}, \tag{2.13}$$
$$|u - \mathcal{I}_{T,N}u|_{m,T} \le CT^{r-m} N^{2m-\frac{1}{2}-r}|u|_{r,T}. \tag{2.14}$$

For analysis, we need to bound the discrete norm by the continuous norm as stated below ([56, Lemma 2.1]).

Lemma 2.2. *For any $\psi \in \mathcal{P}_{N+1}(0,T)$, there holds*

$$\|\psi\|_{T,N} \le \gamma_1 \|\psi\|_T, \tag{2.15}$$

where $\gamma_1 = \sqrt{2 + \frac{2}{2N+1}}$.

The following estimate can be proved by using similar techniques as in Lemma 2.2.

Lemma 2.3. *For any $\psi \in \mathcal{P}_{N+2}(0,T)$, there holds*

$$\|\psi\|_{T,N} \le \gamma_2 \|\psi\|_T, \tag{2.16}$$

where $\gamma_2 = \sqrt{3 + \frac{78}{2N-1}}$.

Proof. Let $\varphi(x) = \psi\left(\frac{T}{2}(x+1)\right)$ with $x \in \Lambda$, then $\varphi \in \mathcal{P}_{N+2}(\Lambda)$. We shall show that

$$\|\varphi\|_N \le \gamma_2 \|\varphi\|. \tag{2.17}$$

To this end, we expand φ and its LGR interpolation as

$$\varphi(x) = \sum_{l=0}^{N+2} \widehat{\varphi}_l L_l(x), \quad \mathcal{I}_N\varphi(x) = \sum_{l=0}^{N} \widetilde{\varphi}_l L_l(x). \tag{2.18}$$

Clearly, $\mathcal{I}_N \varphi L_l \in \mathcal{P}_{N+l}(-1,1)$, by (2.4) we have

$$\begin{aligned} \widetilde{\varphi}_l =& \frac{2l+1}{2}\left(\mathcal{I}_N\varphi, L_l\right) = \frac{2l+1}{2}\left(\mathcal{I}_N\varphi, L_l\right)_N \\ =& \frac{2l+1}{2}\left(\varphi, L_l\right)_N = \widehat{\varphi}_l, \quad 0 \le l \le N-2. \end{aligned} \tag{2.19}$$

Noting that $L_{N+1}(x_j^N) - L_N(x_j^N) = 0$ for $0 \le j \le N$, then using (2.1), (2.2), (2.4) and (2.18) gives

$$\begin{aligned} \widetilde{\varphi}_{N-1} &= \frac{2N-1}{2}\left(\mathcal{I}_N\varphi, L_{N-1}\right) = \frac{2N-1}{2}\left(\mathcal{I}_N\varphi, L_{N-1}\right)_N = \frac{2N-1}{2}\left(\varphi, L_{N-1}\right)_N \\ &= \frac{2N-1}{2}\left(\widehat{\varphi}_{N-1}L_{N-1}, L_{N-1}\right) + \frac{2N-1}{2}\left(\widehat{\varphi}_{N+2}L_{N+2}, L_{N-1}\right)_N \\ &= \widehat{\varphi}_{N-1} + \frac{2N-1}{2}\left(\widehat{\varphi}_{N+2}\left(\frac{2N+3}{N+2}xL_{N+1} - \frac{N+1}{N+2}L_N\right), L_{N-1}\right)_N \\ &= \widehat{\varphi}_{N-1} + \frac{2N-1}{2}\left(\widehat{\varphi}_{N+2}\frac{2N+3}{N+2}x\left(L_{N+1}-L_N\right) + \widehat{\varphi}_{N+2}\frac{2N+3}{N+2}xL_N, L_{N-1}\right)_N \\ &= \widehat{\varphi}_{N-1} + \frac{2N-1}{2}\left(\widehat{\varphi}_{N+2}\frac{2N+3}{N+2}xL_N, L_{N-1}\right)_N \\ &= \widehat{\varphi}_{N-1} + \frac{2N-1}{2}\left(\widehat{\varphi}_{N+2}\frac{2N+3}{N+2}\left(\frac{N+1}{2N+1}L_{N+1} + \frac{N}{2N+1}L_{N-1}\right), L_{N-1}\right)_N \\ &= \widehat{\varphi}_{N-1} + \frac{N(2N+3)}{(N+2)(2N+1)}\widehat{\varphi}_{N+2} \end{aligned}$$

and

$$\begin{aligned} \widetilde{\varphi}_N &= \frac{2N+1}{2}\left(\mathcal{I}_N\varphi, L_N\right) = \frac{2N+1}{2}\left(\varphi, L_N\right)_N \\ &= \frac{2N+1}{2}\left(\widehat{\varphi}_N L_N, L_N\right) + \frac{2N+1}{2}\left(\widehat{\varphi}_{N+1}L_{N+1} + \widehat{\varphi}_{N+2}L_{N+2}, L_N\right)_N \\ &= \widehat{\varphi}_N + \widehat{\varphi}_{N+1} + \frac{2N+1}{2}\left(\widehat{\varphi}_{N+2}L_{N+2}, L_N\right)_N \\ &= \widehat{\varphi}_N + \widehat{\varphi}_{N+1} + \frac{2N+1}{2}\left(\widehat{\varphi}_{N+2}\left(\frac{2N+3}{N+2}x(L_{N+1} - L_N + L_N) - \frac{N+1}{N+2}L_N\right), L_N\right)_N \\ &= \widehat{\varphi}_N + \widehat{\varphi}_{N+1} + \frac{2N+1}{2}\left(\widehat{\varphi}_{N+2}\left(\frac{2N+3}{N+2}xL_N - \frac{N+1}{N+2}L_N\right), L_N\right)_N \end{aligned}$$

$$= \widehat{\varphi}_N + \widehat{\varphi}_{N+1} - \frac{N+1}{N+2}\widehat{\varphi}_{N+2} + \frac{2N+1}{2}\left(\frac{(2N+3)(N+1)}{(2N+1)(N+2)}\widehat{\varphi}_{N+2}L_{N+1}, L_N\right)_N$$
$$= \widehat{\varphi}_N + \widehat{\varphi}_{N+1} + \frac{2(N+1)}{(2N+1)(N+2)}\widehat{\varphi}_{N+2},$$

which together with (2.18) and (2.19) leads to

$$\begin{aligned}
\|\mathcal{I}_N\varphi\|^2 = \sum_{l=0}^{N}\frac{2}{2l+1}\widetilde{\varphi}_l^2 \le{}& \sum_{l=0}^{N-2}\frac{2}{2l+1}\widehat{\varphi}_l^2 + \frac{2}{2N-1}\left(\widehat{\varphi}_{N-1} + \frac{N(2N+3)}{(N+2)(2N+1)}\widehat{\varphi}_{N+2}\right)^2 \\
&+ \frac{2}{2N+1}\left(\widehat{\varphi}_N + \widehat{\varphi}_{N+1} + \frac{2(N+1)}{(2N+1)(N+2)}\widehat{\varphi}_{N+2}\right)^2 \\
\le{}& \sum_{l=0}^{N-2}\frac{2}{2l+1}\widehat{\varphi}_l^2 + \frac{4}{2N-1}\widehat{\varphi}_{N-1}^2 + \frac{4}{2N-1}\left(\frac{N(2N+3)}{(N+2)(2N+1)}\right)^2\widehat{\varphi}_{N+2}^2 \\
&+ \frac{6}{2N+1}\widehat{\varphi}_N^2 + \frac{6}{2N+1}\widehat{\varphi}_{N+1}^2 + \frac{6}{2N+1}\left(\frac{2(N+1)}{(N+2)(2N+1)}\right)^2\widehat{\varphi}_{N+2}^2 \\
\le{}& \sum_{l=0}^{N+2}\frac{2}{2l+1}\widehat{\varphi}_l^2 + \sum_{l=N-1}^{N+2}\frac{2}{2l+1}\widehat{\varphi}_l^2 + \sum_{l=N}^{N+1}\frac{2}{2l+1}\widehat{\varphi}_l^2 + \frac{6}{(2N+1)}\frac{2}{(2N+3)}\widehat{\varphi}_{N+1}^2 \\
&+ 12\left(\frac{1}{2N-1} + \frac{2N+5}{(2N+1)^3}\right)\frac{2}{(2N+5)}\widehat{\varphi}_{N+2}^2 \\
\le{}& \left(3 + \frac{6}{2N+1} + 12\left(\frac{1}{2N-1} + \frac{2N+5}{(2N+1)^3}\right)\right)\|\varphi\|^2,
\end{aligned}$$

and thus

$$\|\mathcal{I}_N\varphi\| \le \sqrt{3 + \frac{78}{2N-1}}\|\varphi\|. \tag{2.20}$$

Moreover, by (2.4) we have

$$\|\varphi\|_N = \|\mathcal{I}_N\varphi\|_N = \|\mathcal{I}_N\varphi\|,$$

which together with (2.20) implies (2.17). Thus, a simple variable transformation of (2.17) leads to (2.16). This completes the proof. $\square$

2.2. Single-interval Legendre-Gauss-Radau collocation scheme

The single-interval LGR collocation scheme for solving (1.1) is to find $u^N(t) \in \mathcal{P}_{N+2}(0,T)$ such that

$$\begin{cases}\partial_t^2 u^N(t_{T,j}^N) = f\left(\partial_t u^N(t_{T,j}^N), u^N(t_{T,j}^N), t_{T,j}^N\right), & 0 \le j \le N, \\ \partial_t u^N(0) = v_0, \quad u^N(0) = u_0. \end{cases} \tag{2.21}$$

Due to (2.9), we observe that

$$\mathcal{I}_{T,N} f\left(\partial_t u^N(t_{T,j}^N), u^N(t_{T,j}^N), t_{T,j}^N\right) = f\left(\partial_t u^N(t_{T,j}^N), u^N(t_{T,j}^N), t_{T,j}^N\right).$$

Then, by (2.21) we have

$$\partial_t^2 u^N\left(t_{T,j}^N\right) = \mathcal{I}_{T,N} f\left(\partial_t u^N(t_{T,j}^N), u^N(t_{T,j}^N), t_{T,j}^N\right), \quad 0 \le j \le N.$$

Since both functions $\partial_t^2 u^N$ and $\mathcal{I}_{T,N} f$ belong to the polynomial space $\mathcal{P}_N(0,T)$, and they have same values at the $N+1$ distinct collocation points. Then, the collocation scheme (2.21) can be reformulated as: Find $u^N(t) \in \mathcal{P}_{N+2}(0,T)$ such that

$$\partial_t^2 u^N(t) = \mathcal{I}_{T,N} f\left(\partial_t u^N(t), u^N(t), t\right), \quad t \in (0,T]. \tag{2.22}$$

We expand the LGR collocation approximation and its derivative by

$$u^N(t) = \sum_{k=0}^{N+2} \widehat{u}_k L_{T,k}(t), \quad \partial_t u^N(t) = \sum_{k=1}^{N+2} \widehat{u}_k \partial_t L_{T,k}(t) \tag{2.23}$$

and let

$$\mathcal{I}_{T,N} f\left(\partial_t u^N(t), u^N(t), t\right) = \sum_{k=0}^{N} \widehat{f}_k L_{T,k}(t). \tag{2.24}$$

Due to (2.12), there holds

$$\widehat{f}_k = \frac{2k+1}{T} \sum_{j=0}^{N} f\left(\partial_t u^N(t_{T,j}^N), u^N(t_{T,j}^N), t_{T,j}^N\right) L_{T,k}\left(t_{T,j}^N\right) \omega_{T,j}^N, \quad 0 \le k \le N. \tag{2.25}$$

Using (2.22)-(2.24) and properties of the shifted Legendre polynomials, a direct computation reveals that ([54])

$$\begin{aligned}\partial_t^2 u^N(t) &= \sum_{k=2}^{N+2} \widehat{u}_k \partial_t^2 L_{T,k}(t) = \sum_{k=0}^{N} \widehat{f}_k L_{T,k}(t) = \sum_{k=1}^{N+1} \tilde{f}_k \partial_t L_{T,k}(t) \\ &= \frac{T\tilde{f}_{N+1}}{2(2N+3)} \partial_t^2 L_{T,N+2}(t) + \frac{T\tilde{f}_N}{2(2N+1)} \partial_t^2 L_{T,N+1}(t) \\ &\quad + \frac{T}{2} \sum_{k=2}^{N} \left(\frac{\tilde{f}_{k-1}}{2k-1} - \frac{\tilde{f}_{k+1}}{2k+3} \right) \partial_t^2 L_{T,k}(t),\end{aligned} \tag{2.26}$$

where

$$\tilde{f}_{N+1} = \frac{T\widehat{f}_N}{2(2N+1)}, \quad \tilde{f}_N = \frac{T\widehat{f}_{N-1}}{2(2N-1)}, \quad \tilde{f}_k = \frac{T}{2}\left(\frac{\widehat{f}_{k-1}}{2k-1} - \frac{\widehat{f}_{k+1}}{2k+3} \right), \quad 1 \le k \le N-1. \tag{2.27}$$

In view of (2.26), comparing the expansion coefficients in terms of $\partial_t^2 L_{T,k}(t)$ leads to

$$\widehat{u}_{N+2} = \frac{T\tilde{f}_{N+1}}{2(2N+3)}, \quad \widehat{u}_{N+1} = \frac{T\tilde{f}_N}{2(2N+1)}, \quad \widehat{u}_k = \frac{T}{2}\left(\frac{\tilde{f}_{k-1}}{2k-1} - \frac{\tilde{f}_{k+1}}{2k+3} \right), \quad 2 \le k \le N. \tag{2.28}$$

Inserting (2.27) into (2.28), we further obtain

$$\widehat{u}_{N+2} = \frac{T^2}{4(2N+3)(2N+1)} \widehat{f}_N, \tag{2.29a}$$

$$\widehat{u}_{N+1} = \frac{T^2}{4(2N+1)(2N-1)} \widehat{f}_{N-1}, \qquad N \ge 1, \tag{2.29b}$$

$$\widehat{u}_N = \frac{T^2}{4(2N-1)(2N-3)} \widehat{f}_{N-2} - \frac{T^2}{2(2N+3)(2N-1)} \widehat{f}_N, \qquad N \ge 2, \tag{2.29c}$$

$$\widehat{u}_{N-1} = \frac{T^2}{4(2N-3)(2N-5)} \widehat{f}_{N-3} - \frac{T^2}{2(2N+1)(2N-3)} \widehat{f}_{N-1}, \quad N \ge 3, \tag{2.29d}$$

$$\widehat{u}_k = \frac{T^2}{4(2k-1)(2k-3)}\widehat{f}_{k-2} - \frac{T^2}{2(2k+3)(2k-1)}\widehat{f}_k + \frac{T^2}{4(2k+5)(2k+3)}\widehat{f}_{k+2} \tag{2.29e}$$

for $2 \le k \le N-2$. Moreover, substituting $t=0$ into the second equality of (2.23), then using (2.21) and the fact $\partial_t L_{T,k}(0) = \frac{1}{T}(-1)^{k-1}k(k+1)$ gives

$$\widehat{u}_1 = \frac{T}{2}v_0 + \frac{1}{2}\sum_{k=2}^{N+2}(-1)^k k(k+1)\widehat{u}_k. \tag{2.30}$$

On the other hand, inserting $t=0$ into (2.23), using (2.21), (2.30) and the fact $L_{T,k}(0) = (-1)^k$, we obtain

$$\widehat{u}_0 = u_0 - \sum_{k=1}^{N+2}(-1)^k\widehat{u}_k = u_0 + \frac{T}{2}v_0 + \frac{1}{2}\sum_{k=2}^{N+2}(-1)^k(k-1)(k+2)\widehat{u}_k. \tag{2.31}$$

Thanks to (2.29)-(2.31), we can compute the expansion coefficients $\{\widehat{u}_k\}_{k=0}^{N+2}$ of the LGR collocation approximation u^N by a simple iterative algorithm, as described in Algorithm 2.1.

Algorithm 2.1. A Simple Iterative Algorithm

1: Input: initial guess of $\{\widehat{u}_k\}_{k=0}^{N+2}$ and tolerance.
2: **while** the maximum absolute difference between two consecutive coefficients of $\{\widehat{u}_k\}_{k=0}^{N+2}$ is bigger than the desired tolerance **do**
3: Compute the coefficients $\{\widehat{f}_k\}_{k=0}^{N}$ by (2.23) and (2.25).
4: Update the coefficients $\{\widehat{u}_k\}_{k=0}^{N+2}$ by (2.29), (2.30) and (2.31).
5: **end while**
6: Output: quantities of interest, such as $u^N(t_{T,j}^N)$, $\partial_t u^N(t_{T,j}^N)$ and $u^N(T)$.

2.3. Convergence analysis

The aim of this subsection is to analyze the convergence of the single-interval LGR collocation scheme (2.21). To this end, we set

$$E^N(t) = \mathcal{I}_{T,N}u(t) - u^N(t).$$

We further define

$$\begin{aligned}
G_{T,1}^N(t) &= \partial_t^2\mathcal{I}_{T,N}u(t) - \mathcal{I}_{T,N}\partial_t^2 u(t),\\
G_{T,2}^N(t) &= f(\partial_t\mathcal{I}_{T,N}u(t), u^N(t), t) - f(\partial_t u^N(t), u^N(t), t),\\
G_{T,3}^N(t) &= f(\partial_t\mathcal{I}_{T,N}u(t), \mathcal{I}_{T,N}u(t), t) - f(\partial_t\mathcal{I}_{T,N}u(t), u^N(t), t),\\
G_{T,4}^N(t) &= f(\mathcal{I}_{T,N}\partial_t u(t), \mathcal{I}_{T,N}u(t), t) - f(\partial_t\mathcal{I}_{T,N}u(t), \mathcal{I}_{T,N}u(t), t).
\end{aligned}$$

Due to (1.1) and the definition of $\mathcal{I}_{T,N}u$, there holds

$$\mathcal{I}_{T,N}\partial_t^2 u(t_{T,j}^N) = \partial_t^2 u(t_{T,j}^N) = f\left(\partial_t u(t_{T,j}^N), u(t_{T,j}^N), t_{T,j}^N\right) = f\left(\mathcal{I}_{T,N}\partial_t u(t_{T,j}^N), \mathcal{I}_{T,N}u(t_{T,j}^N), t_{T,j}^N\right)$$

for $0 \le j \le N$, and then we have

$$\partial_t^2\mathcal{I}_{T,N}u(t_{T,j}^N) = f\left(\partial_t u(t_{T,j}^N), u(t_{T,j}^N), t_{T,j}^N\right) + G_{T,1}^N(t_{T,j}^N), \quad 0 \le j \le N. \tag{2.32}$$

Combining (2.21) and (2.32) yields

$$\begin{cases} \partial_t^2 E^N(t_{T,j}^N) = \sum_{j=1}^{4} G_{T,j}^N(t_{T,j}^N), \quad 0 \le j \le N, \\ \partial_t E^N(0) = \partial_t \mathcal{I}_{T,N} u(0) - v_0, \quad E^N(0) = \mathcal{I}_{T,N} u(0) - u_0. \end{cases} \tag{2.33}$$

For our purpose, we assume that f in (1.1) is continuous and satisfies uniform Lipschitz conditions, i.e., there exist positive constants L_1 and L_2 such that

$$|f(z_1, s, t) - f(z_2, s, t)| \le L_1 |z_1 - z_2|, \quad |f(z, s_1, t) - f(z, s_2, t)| \le L_2 |s_1 - s_2| \tag{2.34}$$

for $t \in (0, T]$, $|z_i| < \infty$ and $|s_i| < \infty$ $(i = 1, 2)$.

The following estimates will be used to deal with the term E^N.

Lemma 2.4. *Let $u \in H^r(0, T)$ with integer $3 \le r \le N + 1$. Then we have*

$$\|G_{T,1}^N\|_{T,N} \le CT^{r-2} N^{\frac{7}{2}-r} |u|_{r,T}, \tag{2.35}$$

$$\|G_{T,2}^N\|_{T,N} \le L_1 \gamma_1 \|\partial_t E^N\|_T, \tag{2.36}$$

$$\|G_{T,3}^N\|_{T,N} \le L_2 \gamma_2 \|E^N\|_T, \tag{2.37}$$

$$\|G_{T,4}^N\|_{T,N} \le CL_1 T^{r-1} N^{\frac{3}{2}-r} |u|_{r,T} \tag{2.38}$$

with $C > 0$ independent on T and N.

Proof. In view of (2.13), there holds for any integer $3 \le r \le N + 3$,

$$\|\partial_t^2 u - \mathcal{I}_{T,N} \partial_t^2 u\|_T \le CT^{r-2} N^{2-r} |u|_{r,T}.$$

This together with (2.8) and (2.14) gives

$$\|G_{T,1}^N\|_{T,N} = \|G_{T,1}^N\|_T \le \|\partial_t^2 (\mathcal{I}_{T,N} u - u)\|_T + \|\partial_t^2 u - \mathcal{I}_{T,N} \partial_t^2 u\|_T \le CT^{r-2} N^{\frac{7}{2}-r} |u|_{r,T}$$

for any integer $3 \le r \le N + 1$. Thus the proof of (2.35) is complete.

Combining (2.34) and (2.15) gives

$$\|G_{T,2}^N\|_{T,N} \le L_1 \|\partial_t \mathcal{I}_{T,N} u - \partial_t u^N\|_{T,N} = L_1 \|\partial_t E^N\|_{T,N} \le L_1 \gamma_1 \|\partial_t E^N\|_T$$

upon noting that $\partial_t E^N \in \mathcal{P}_{N+1}(0, T)$. This proves (2.36).

Since $E^N \in \mathcal{P}_{N+2}(0, T)$, applying (2.34) and (2.16) yields

$$\|G_{T,3}^N\|_{T,N} \le L_2 \|\mathcal{I}_{T,N} u - u^N\|_{T,N} = L_2 \|E^N\|_{T,N} \le L_2 \gamma_2 \|E^N\|_T,$$

which implies (2.37).

Moreover, using (2.34), (2.13) and (2.14) we deduce that

$$\begin{aligned} \|G_{T,4}^N\|_{T,N} &\le L_1 \|\mathcal{I}_{T,N} \partial_t u - \partial_t \mathcal{I}_{T,N} u\|_{T,N} \\ &\le L_1 \left(\|\mathcal{I}_{T,N} \partial_t u - \partial_t u\|_{T,N} + \|\partial_t u - \partial_t \mathcal{I}_{T,N} u\|_{T,N} \right) \\ &\le CL_1 T^{r-1} N^{\frac{3}{2}-r} |u|_{r,T}. \end{aligned}$$

This completes the proof of (2.38). □

We now estimate E^N.

Lemma 2.5. *Let $u \in H^r(0,T)$ with integer $3 \le r \le N+1$. Then we have*

$$\|\partial_t E^N(t) - \partial_t E^N(0)\|_T \le 2T\left(L_1\gamma_1\|\partial_t E^N\|_T + L_2\gamma_2\|E^N\|_T + CC_*T^{r-2}N^{\frac{7}{2}-r}|u|_{r,T}\right), \quad (2.39)$$

$$|\partial_t E^N(T) - \partial_t E^N(0)| \le 2T^{\frac{1}{2}}\left(L_1\gamma_1\|\partial_t E^N\|_T + L_2\gamma_2\|E^N\|_T + CC_*T^{r-2}N^{\frac{7}{2}-r}|u|_{r,T}\right), \quad (2.40)$$

where $C_* = 1 + L_1TN^{-2}$ and $C > 0$ is independent on T and N.

Proof. For simplicity, we denote $E_1(t) = \partial_t E^N(t) - \partial_t E^N(0)$ and $C_* = 1 + L_1TN^{-2}$. Then, we have $E_1 \in \mathcal{P}_{N+1}(0,T)$, $t^{-1}E_1 \in \mathcal{P}_N(0,T)$ and $\partial_t(t^{-1}E_1) \in \mathcal{P}_{N-1}(0,T)$. By (2.8) and integration by parts, we get

$$\begin{aligned} 2\left(E_1, \partial_t(t^{-1}E_1)\right)_{T,N} &= 2\left(E_1, \partial_t(t^{-1}E_1)\right)_T \\ &= -2\left(E_1, t^{-2}E_1\right)_T + 2\left(E_1, t^{-1}\partial_t E_1\right)_T \\ &= -2\|t^{-1}E_1\|_T^2 + \left(t^{-1}, \partial_t(E_1^2)\right)_T \\ &= -\|t^{-1}E_1\|_T^2 + T^{-1}|E_1(T)|^2. \end{aligned} \quad (2.41)$$

On the other hand, by (2.8) and (2.33) we obtain

$$\begin{aligned} 2\left(E_1, \partial_t(t^{-1}E_1)\right)_{T,N} &= -2(E_1, t^{-2}E_1)_{T,N} + 2(E_1, t^{-1}\partial_t^2 E^N)_{T,N} \\ &= -2\|t^{-1}E_1\|_T^2 + 2\left(t^{-1}E_1, \sum_{j=1}^{4} G_{T,j}^N\right)_{T,N}. \end{aligned} \quad (2.42)$$

Combining (2.41) and (2.42) gives

$$\|t^{-1}E_1\|_T^2 + T^{-1}|E_1(T)|^2 = \sum_{j=1}^{4} 2\left(t^{-1}E_1, G_{T,j}^N\right)_{T,N} =: \sum_{j=1}^{4} A_{T,j}^N. \quad (2.43)$$

Since $t^{-1}E_1 \in \mathcal{P}_N(0,T)$, applying (2.8) yields

$$|A_{T,j}^N| = 2\left|\left(t^{-1}E_1, G_{T,j}^N\right)_{T,N}\right| \le 2\|t^{-1}E_1\|_T\|G_{T,j}^N\|_{T,N}, \quad 1 \le j \le 4. \quad (2.44)$$

Thus, by (2.43) and (2.44) we get

$$\|t^{-1}E_1\|_T^2 \le \sum_{j=1}^{4} A_{T,j}^N \le 2\|t^{-1}E_1\|_T \sum_{j=1}^{4} \|G_{T,j}^N\|_{T,N}. \quad (2.45)$$

Applying Lemma 2.4 to (2.45) gives

$$\begin{aligned} \|t^{-1}E_1\|_T &\le 2\sum_{j=1}^{4} \|G_{T,j}^N\|_{T,N} \\ &\le 2\left(L_1\gamma_1\|\partial_t E^N\|_T + L_2\gamma_2\|E^N\|_T + CC_*T^{r-2}N^{\frac{7}{2}-r}|u|_{r,T}\right), \end{aligned} \quad (2.46)$$

which implies that

$$\|E_1\|_T \le T\|t^{-1}E_1\|_T \le 2T\left(L_1\gamma_1\|\partial_t E^N(t)\|_T + L_2\gamma_2\|E^N(t)\|_T + CC_*T^{r-2}N^{\frac{7}{2}-r}|u|_{r,T}\right).$$

This completes the proof of (2.39).

Moreover, thanks to (2.43), (2.45) and (2.46), we find that

$$T^{-1}|E_1(T)|^2 \le \sum_{j=1}^{4} A_{T,j}^N \quad \le 2\|t^{-1}E_1\|_T \sum_{j=1}^{4} \|G_{T,j}^N\|_{T,N} \le 4\left(\sum_{j=1}^{4} \|G_{T,j}^N\|_{T,N}\right)^2,$$

which together with Lemma 2.4 leads to

$$|E_1(T)| \le 2T^{\frac{1}{2}}\left(L_1\gamma_1\|\partial_t E^N(t)\|_T + L_2\gamma_2\|E^N(t)\|_T + CC_* T^{r-2}N^{\frac{7}{2}-r}|u|_{r,T}\right).$$

This completes the proof of (2.40). □

We are ready to present the main results of this section.

Theorem 2.1. *Let $u \in H^r(0,T)$ with integer $3 \le r \le N+1$. Assume that T is suitably small and there exist positive constants α and β such that*

$$2TL_1\gamma_1 \le \alpha < 1 \quad \text{and} \quad \frac{4T^2L_2\gamma_2}{1-2TL_1\gamma_1} \le \beta < 1. \tag{2.47}$$

Then, we have

$$\|u-u^N\|_T \le C_{\alpha,\beta}C_*T^rN^{\frac{7}{2}-r}|u|_{r,T}, \tag{2.48}$$

$$\|\partial_t u-\partial_t u^N\|_T \le C_{\alpha,\beta}C_*T^{r-1}N^{\frac{7}{2}-r}|u|_{r,T}, \tag{2.49}$$

$$|u(T)-u^N(T)| \le C_{\alpha,\beta}C_*T^{r-\frac{1}{2}}N^{\frac{7}{2}-r}|u|_{r,T}, \tag{2.50}$$

$$|\partial_t u(T)-\partial_t u^N(T)| \le C_{\alpha,\beta}C_*T^{r-\frac{3}{2}}N^{\frac{7}{2}-r}|u|_{r,T}, \tag{2.51}$$

where $C_*>0$ is defined as in Lemma 2.5 and $C_{\alpha,\beta}>0$ depends on α,β but not on T,N.

Proof. Noting that for any $v \in H^1(0,T)$, there holds (page 279 of [21]),

$$\max_{t\in[0,T]} |v(t)| \le T^{-\frac{1}{2}}\|v\|_T + T^{\frac{1}{2}}\|\partial_t v\|_T. \tag{2.52}$$

This together with (2.33) and (2.14) yields

$$\begin{aligned}|\partial_t E^N(0)| &= |\partial_t \mathcal{I}_{T,N}u(0) - \partial_t u(0)| \\ &\le T^{-\frac{1}{2}}\|\partial_t(\mathcal{I}_{T,N}u-u)\|_T + T^{\frac{1}{2}}\|\partial_t^2(\mathcal{I}_{T,N}u-u)\|_T \\ &\le CT^{r-\frac{3}{2}}N^{\frac{7}{2}-r}|u|_{r,T}.\end{aligned} \tag{2.53}$$

Similarly, applying Lemma 2.1 we obtain

$$\begin{aligned}|E^N(0)| &= |\mathcal{I}_{T,N}u(0) - u(0)| \\ &\le T^{-\frac{1}{2}}\|\mathcal{I}_{T,N}u-u\|_T + T^{\frac{1}{2}}\|\partial_t(\mathcal{I}_{T,N}u-u)\|_T \\ &\le CT^{r-\frac{1}{2}}N^{\frac{3}{2}-r}|u|_{r,T}.\end{aligned} \tag{2.54}$$

Combining (2.39) and (2.53) gives

$$\begin{aligned}\|\partial_t E^N\|_T &\le \|\partial_t E^N(t) - \partial_t E^N(0)\|_T + \|\partial_t E^N(0)\|_T \\ &= \|\partial_t E^N(t) - \partial_t E^N(0)\|_T + T^{\frac{1}{2}}|\partial_t E^N(0)| \\ &\le 2T\left(L_1\gamma_1\|\partial_t E^N\|_T + L_2\gamma_2\|E^N\|_T + CC_*T^{r-2}N^{\frac{7}{2}-r}|u|_{r,T}\right),\end{aligned}$$

or equivalently,

$$(1 - 2TL_1\gamma_1)\|\partial_t E^N\|_T \le 2TL_2\gamma_2\|E^N\|_T + CC_*T^{r-1}N^{\frac{7}{2}-r}|u|_{r,T}. \tag{2.55}$$

Suppose that T is suitably small and there is a positive constant α such that

$$2TL_1\gamma_1 \le \alpha < 1. \tag{2.56}$$

Then, we can rewrite (2.55) as

$$\|\partial_t E^N\|_T \le \frac{2TL_2\gamma_2}{1-2TL_1\gamma_1}\|E^N\|_T + CC_*\frac{1}{1-2TL_1\gamma_1}T^{r-1}N^{\frac{7}{2}-r}|u|_{r,T}. \tag{2.57}$$

Upon observing that

$$|E^N(t)|^2 - |E^N(0)|^2 = 2\int_0^t \partial_t E^N E^N dt \le 2\|E^N\|_T\|\partial_t E^N\|_T$$

and integrating the above inequality with respect to t over the interval $(0,T)$, we get

$$\|E^N\|_T^2 \le T|E^N(0)|^2 + 2T\|E^N\|_T\|\partial_t E^N\|_T \le T|E^N(0)|^2 + \frac{1}{2}\|E^N\|_T^2 + 2T^2\|\partial_t E^N\|_T^2,$$

which implies that

$$\|E^N\|_T \le \sqrt{2}T^{\frac{1}{2}}|E^N(0)| + 2T\|\partial_t E^N\|_T. \tag{2.58}$$

Inserting (2.54) and (2.57) into (2.58) gives

$$\|E^N\|_T \le CT^rN^{\frac{3}{2}-r}|u|_{r,T} + \frac{4T^2L_2\gamma_2}{1-2TL_1\gamma_1}\|E^N\|_T + CC_*\frac{1}{1-2TL_1\gamma_1}T^rN^{\frac{7}{2}-r}|u|_{r,T},$$

or equivalently, thanks to (2.56), we have

$$\left(1 - \frac{4T^2L_2\gamma_2}{1-2TL_1\gamma_1}\right)\|E^N\|_T \le C_\alpha C_*T^rN^{\frac{7}{2}-r}|u|_{r,T}, \tag{2.59}$$

where $C_\alpha > 0$ depends on α and possibly having different values in each occurrence. Suppose that T is suitably small and there is a positive constant β such that

$$\frac{4T^2L_2\gamma_2}{1-2TL_1\gamma_1} \le \beta < 1. \tag{2.60}$$

Then, (2.59) can be read as

$$\|E^N\|_T \le C_{\alpha,\beta}C_*T^rN^{\frac{7}{2}-r}|u|_{r,T}. \tag{2.61}$$

Here, $C_{\alpha,\beta} > 0$ depends on α, β and possibly having different values in each occurrence. Applying the triangle inequality, using (2.13) and (2.61), we obtain

$$\|u - u^N\|_T \le \|u - \mathcal{I}_{T,N}u\|_T + \|E^N\|_T \le C_{\alpha,\beta}C_*T^rN^{\frac{7}{2}-r}|u|_{r,T}.$$

This completes the proof of (2.48). Inserting (2.61) into (2.57), then using (2.56) and (2.60) gives

$$\begin{aligned}\|\partial_t E^N\|_T &\le \frac{2TL_2\gamma_2}{1-2TL_1\gamma_1}C_{\alpha,\beta}C_*T^rN^{\frac{7}{2}-r}|u|_{r,T} + CC_*\frac{1}{1-2TL_1\gamma_1}T^{r-1}N^{\frac{7}{2}-r}|u|_{r,T}\\ &\le \frac{2T^2L_2\gamma_2}{1-2TL_1\gamma_1}C_{\alpha,\beta}C_*T^{r-1}N^{\frac{7}{2}-r}|u|_{r,T} + C_\alpha C_*T^{r-1}N^{\frac{7}{2}-r}|u|_{r,T}\end{aligned}$$

$$\leq \frac{\beta}{2} C_{\alpha,\beta} C_* T^{r-1} N^{\frac{7}{2}-r} |u|_{r,T} + C_\alpha C_* T^{r-1} N^{\frac{7}{2}-r} |u|_{r,T}$$
$$\leq C_{\alpha,\beta} C_* T^{r-1} N^{\frac{7}{2}-r} |u|_{r,T}. \tag{2.62}$$

Applying the triangle inequality, using (2.14) and (2.62), we get

$$\|\partial_t u - \partial_t u^N\|_T \leq \|\partial_t (u - \mathcal{I}_{T,N} u)\|_T + \|\partial_t E^N\|_T \leq C_{\alpha,\beta} C_* T^{r-1} N^{\frac{7}{2}-r} |u|_{r,T}.$$

This proves (2.49). Since $u(T) = \mathcal{I}_{T,N} u(T)$, there holds $u(T) - u^N(T) = E^N(T)$. Then, thanks to (2.52), combining (2.61) and (2.62), we obtain

$$|u(T) - u^N(T)| = |E^N(T)| \leq T^{-\frac{1}{2}} \|E^N\|_T + T^{\frac{1}{2}} \|\partial_t E^N\|_T \leq C_{\alpha,\beta} C_* T^{r-\frac{1}{2}} N^{\frac{7}{2}-r} |u|_{r,T},$$

which implies (2.50).

Moreover, inserting (2.61) and (2.62) into (2.40), then using (2.56) and (2.60), we obtain

$$\begin{aligned}
|\partial_t E^N(T) - \partial_t E^N(0)| &\leq 2T^{\frac{1}{2}} \Big(\frac{T^2 L_2 \gamma_2}{1 - 2TL_1\gamma_1} (1 - 2TL_1\gamma_1) C_{\alpha,\beta} C_* T^{r-2} N^{\frac{7}{2}-r} |u|_{r,T} \\
&\qquad + TL_1\gamma_1 C_{\alpha,\beta} C_* T^{r-2} N^{\frac{7}{2}-r} |u|_{r,T} + C C_* T^{r-2} N^{\frac{7}{2}-r} |u|_{r,T} \Big) \\
&\leq 2T^{\frac{1}{2}} \Big(\frac{\beta}{4} C_{\alpha,\beta} C_* T^{r-2} N^{\frac{7}{2}-r} |u|_{r,T} + TL_1\gamma_1 C_{\alpha,\beta} C_* T^{r-2} N^{\frac{7}{2}-r} |u|_{r,T} \\
&\qquad + C C_* T^{r-2} N^{\frac{7}{2}-r} |u|_{r,T} \Big) \\
&\leq C_{\alpha,\beta} C_* T^{r-\frac{3}{2}} N^{\frac{7}{2}-r} |u|_{r,T},
\end{aligned}$$

which together with (2.53) gives

$$|\partial_t E^N(T)| \leq |\partial_t E^N(T) - \partial_t E^N(0)| + |\partial_t E^N(0)| \leq C_{\alpha,\beta} C_* T^{r-\frac{3}{2}} N^{\frac{7}{2}-r} |u|_{r,T}. \tag{2.63}$$

Applying the triangle inequality, using (2.52), (2.14) and (2.63), we deduce that

$$\begin{aligned}
|\partial_t u(T) - \partial_t u^N(T)| &\leq |\partial_t u(T) - \partial_t \mathcal{I}_{T,N} u(T)| + |\partial_t E^N(T)| \\
&\leq T^{-\frac{1}{2}} \|\partial_t (u - \mathcal{I}_{T,N} u)\|_T + T^{\frac{1}{2}} \|\partial_t^2 (u - \mathcal{I}_{T,N} u)\|_T + |\partial_t E^N(T)| \\
&\leq C_{\alpha,\beta} C_* T^{r-\frac{3}{2}} N^{\frac{7}{2}-r} |u|_{r,T}.
\end{aligned}$$

This proves (2.51). □

Remark 2.1. The error estimates (2.48)-(2.51) imply that the convergence rate of the single-interval LGR collocation method is of the order $\mathcal{O}(N^{\frac{7}{2}-r})$ for fixed T. Clearly, the errors decay rapidly as N and r increase. In other words, the single-interval LGR collocation method can yield arbitrary high-order algebraic convergence rate (i.e., spectral convergence), provided that the solution u is smooth enough.

Remark 2.2. We note that the LG spectral collocation method was developed in [24] for second-order ODEs, where the convergence rate of the numerical errors is of the order $\mathcal{O}(N^{4-r})$ for fixed T provided that $\partial_r u \in L^\infty(0,T)$ (see [24, Remarks 3.3 and 3.6]). Although both methods can achieve spectral convergence, the convergence of our method in N is half order higher than the method proposed in [24]. Moreover, it is well-known that the Gauss-type quadrature formulas provide powerful tools for evaluating integrals and inner products in spectral collocation methods. Since the degrees of precision of the LGR and LG quadrature formulas with

$N+1$ points are $2N$ and $2N+1$, respectively, this leads to different consideration in the error analysis for the spectral collocation methods based on LGR and LG points, and some new technique results (see, e.g., Lemma 2.3) are also needed in our situation for the LGR case.

Remark 2.3. If $\partial_r u \in L^\infty(0,T)$ and $T<1$, then from (2.48)-(2.51) we deduce that

$$\|u-u^N\|_T = \mathcal{O}(T^{r+\frac{1}{2}}N^{\frac{7}{2}-r}), \qquad \|\partial_t u-\partial_t u^N\|_T = \mathcal{O}(T^{r-\frac{1}{2}}N^{\frac{7}{2}-r}),$$
$$|u(T)-u^N(T)| = \mathcal{O}(T^{r}N^{\frac{7}{2}-r}), \quad |\partial_t u(T)-\partial_t u^N(T)| = \mathcal{O}(T^{r-1}N^{\frac{7}{2}-r}).$$

2.4. Multi-interval Legendre-Gauss-Radau collocation scheme

In the last section, we proposed and analyzed a single-interval LGR collocation method, and the theoretical results show that the numerical errors decay rapidly as N and r increase. However, the length of the interval $(0,T)$ is sometimes limited due to the condition (2.47). On the other hand, it is not convenient for us to solve the resulted discrete system with large N. To remedy these deficiencies, we introduce a multi-interval LGR collocation scheme as follows.

For this purpose, we first divide the interval $(0,T]$ into M subintervals $\{I_m := (T_{m-1},T_m]\}_{m=1}^M$ with nodes given by

$$0=T_0<T_1<\cdots<T_M=T.$$

Let $\tau_m := T_m - T_{m-1},\ 1\le m\le M$. We further set $u_m(t) := u(T_{m-1}+t)$ for $0\le t\le \tau_m$. In view of (1.1), there holds

$$\begin{cases} \partial_t^2 u_m(t) = f(\partial_t u_m(t), u_m(t), T_{m-1}+t), & 0<t\le\tau_m, \quad 1\le m\le M, \\ \partial_t u_m(0) = \partial_t u_{m-1}(\tau_{m-1}), \quad u_m(0)=u_{m-1}(\tau_{m-1}), & 2\le m\le M, \\ \partial_t u_1(0)=v_0, \quad u_1(0)=u_0. \end{cases} \tag{2.64}$$

By replacing T and N by τ_1 and N_1 in (2.21), respectively, we can obtain a local approximation $u_1^{N_1}(t)\in\mathcal{P}_{N_1+2}(0,\tau_1)$ for $u_1(t)$ with $\partial_t u_1^{N_1}(0)=v_0$ and $u_1^{N_1}(0)=u_0$. Similarly, we can obtain the local numerical solutions $u_m^{N_m}(t)\in\mathcal{P}_{N_m+2}(0,\tau_m)$ for $2\le m\le M$ by using the time stepping scheme

$$\begin{cases} \partial_t^2 u_m^{N_m}(t_{\tau_m,j}^{N_m}) = f\left(\partial_t u_m^{N_m}(t_{\tau_m,j}^{N_m}), u_m^{N_m}(t_{\tau_m,j}^{N_m}), T_{m-1}+t_{\tau_m,j}^{N_m}\right), & 2\le m\le M, \quad 0\le j\le N_m, \\ \partial_t u_m^{N_m}(0) = \partial_t u_{m-1}^{N_{m-1}}(\tau_{m-1}), \quad u_m^{N_m}(0) = u_{m-1}^{N_{m-1}}(\tau_{m-1}), & 2\le m\le M, \end{cases} \tag{2.65}$$

where $\{t_{\tau_m,k}^{N_m}\}_{k=0}^{N_m}$ are the shifted LGR quadrature nodes on the interval $(0,\tau_m]$. Then, the global numerical solution of (1.1) is given by

$$u^N(T_{m-1}+t) = u_m^{N_m}(t), \quad 0\le t\le\tau_m, \quad 1\le m\le M. \tag{2.66}$$

Clearly, $u_m^{N_m}(t)$ is an approximation to the local exact solution $u_m(t)$ for $1\le m\le M$.

We now turn to the error analysis. For simplicity, we consider the case with uniform mode $N_m=N$ and uniform step-size $\tau_m=\tau$. To this end, we set

$$E_m^N(t) = \mathcal{I}_{\tau,N}u_m(t) - u_m^N(t), \quad 1\le m\le M.$$

We further define

$$_mG_{\tau,1}^N(t) = \partial_t^2\mathcal{I}_{\tau,N}u_m(t) - \mathcal{I}_{\tau,N}\partial_t^2 u_m(t),$$
$$_mG_{\tau,2}^N(t) = f(\partial_t\mathcal{I}_{\tau,N}u_m(t), u_m^N(t), t) - f(\partial_t u_m^N(t), u_m^N(t), t),$$

$$
\begin{aligned}
{}_mG^N_{\tau,3}(t) &= f(\partial_t\mathcal{I}_{\tau,N}u_m(t),\mathcal{I}_{\tau,N}u_m(t),t) - f(\partial_t\mathcal{I}_{\tau,N}u_m(t),u^N_m(t),t),\\
{}_mG^N_{\tau,4}(t) &= f(\mathcal{I}_{\tau,N}\partial_t u_m(t),\mathcal{I}_{\tau,N}u_m(t),t) - f(\partial_t\mathcal{I}_{\tau,N}u_m(t),\mathcal{I}_{\tau,N}u_m(t),t).
\end{aligned}
$$

Following the same line as in the derivation of (2.33), we obtain from (2.64) and (2.65) with $N_m = N$ and $\tau_m = \tau$ that

$$
\begin{cases}
\partial_t^2 E^N_m(t^N_{\tau,j}) = \sum_{j=1}^{4} {}_mG^N_{\tau,j}(t^N_{\tau,j}), \quad 0\le j\le N, \quad 1\le m\le M,\\
\partial_t E^N_m(0) = \partial_t\mathcal{I}_{\tau,N}u_m(0) - \partial_t u^N_{m-1}(\tau),\\
E^N_m(0) = \mathcal{I}_{\tau,N}u_m(0) - u^N_{m-1}(\tau), \qquad\qquad 2\le m\le M,\\
\partial_t E^N_1(0) = \partial_t\mathcal{I}_{\tau,N}u_1(0) - v_0, \quad E^N_1(0) = \mathcal{I}_{\tau,N}u_1(0) - u_0.
\end{cases}
\tag{2.67}
$$

Similar to the proof of Lemma 2.5, we can easily deduce the following results.

Lemma 2.6. *Assume that f satisfies (2.34). Let $u_m \in H^r(0,\tau)$ with integer $3\le r\le N+1$. Then we have*

$$
\|\partial_t E^N_m(t) - \partial_t E^N_m(0)\|_\tau \le C\tau\left(\|\partial_t E^N_m\|_\tau + \|E^N_m\|_\tau + \tau^{r-2}N^{\frac{7}{2}-r}|u_m|_{r,\tau}\right), \tag{2.68}
$$

$$
|\partial_t E^N_m(\tau) - \partial_t E^N_m(0)| \le C\tau^{\frac{1}{2}}\left(\|\partial_t E^N_m\|_\tau + \|E^N_m\|_\tau + \tau^{r-2}N^{\frac{7}{2}-r}|u_m|_{r,\tau}\right), \tag{2.69}
$$

where the constant $C>0$ is independent of τ and N.

The following theorem establishes the spectral convergence of the multi-interval LGR collocation scheme for the problem (1.1).

Theorem 2.2. *Assume that f satisfies (2.34). Let $u\in H^r(0,T)$ with integer $3\le r\le N+1$. Then, for sufficiently small $\tau>0$, there hold*

$$
\|u-u^N\|_{L^2(0,m\tau)} \le Cm\tau^r N^{\frac{7}{2}-r}|u|_{H^r(0,m\tau)}, \tag{2.70}
$$

$$
\|\partial_t u-\partial_t u^N\|^2_{L^2(0,m\tau)} \le Cm\tau^{r-1} N^{\frac{7}{2}-r}|u|_{H^r(0,m\tau)}, \tag{2.71}
$$

$$
|u(m\tau)-u^N(m\tau)| \le Cm^{\frac{1}{2}}\tau^{r-\frac{1}{2}} N^{\frac{7}{2}-r}|u|_{H^r(0,m\tau)}, \tag{2.72}
$$

$$
|\partial_t u(m\tau)-\partial_t u^N(m\tau)| \le Cm^{\frac{1}{2}}\tau^{r-\frac{3}{2}} N^{\frac{7}{2}-r}|u|_{H^r(0,m\tau)} \tag{2.73}
$$

for $1\le m\le M$, where the constant $C>0$ is independent of τ and N.

Proof. According to (2.48)-(2.51), there hold

$$
\|u-u^N\|_{L^2(0,\tau)} = \|u_1-u^N_1\|_\tau \le C\tau^r N^{\frac{7}{2}-r}|u_1|_{r,\tau}, \tag{2.74}
$$

$$
\|\partial_t u-\partial_t u^N\|_{L^2(0,\tau)} = \|\partial_t u_1-\partial_t u^N_1\|_\tau \le C\tau^{r-1} N^{\frac{7}{2}-r}|u_1|_{r,\tau}, \tag{2.75}
$$

$$
|u(\tau)-u^N(\tau)| = |u_1(\tau)-u^N_1(\tau)| \le C\tau^{r-\frac{1}{2}} N^{\frac{7}{2}-r}|u_1|_{r,\tau}, \tag{2.76}
$$

$$
|\partial_t u(\tau)-\partial_t u^N(\tau)| = |\partial_t u_1(\tau)-\partial_t u^N_1(\tau)| \le C\tau^{r-\frac{3}{2}} N^{\frac{7}{2}-r}|u_1|_{r,\tau} \tag{2.77}
$$

for sufficiently small τ.

We next estimate the term E^N_m for $m=2$. Noting the fact that

$$
E^N_2(0) = \mathcal{I}_{\tau,N}u_2(0) - u^N_1(\tau) = (\mathcal{I}_{\tau,N}u_2(0) - u_2(0)) + \left(u_1(\tau) - u^N_1(\tau)\right),
$$

then using (2.54) and (2.76) gives

$$\begin{aligned}|E_2^N(0)| &\le C\tau^{r-\frac{1}{2}}N^{\frac{3}{2}-r}|u_2|_{r,\tau} + C\tau^{r-\frac{1}{2}}N^{\frac{7}{2}-r}|u_1|_{r,\tau}\\ &\le C\tau^{r-\frac{1}{2}}N^{\frac{7}{2}-r}\left(|u_1|_{r,\tau}+|u_2|_{r,\tau}\right).\end{aligned} \tag{2.78}$$

Similarly, due to (2.53) and (2.77), we have

$$\begin{aligned}|\partial_t E_2^N(0)| &\le C\tau^{r-\frac{3}{2}}N^{\frac{7}{2}-r}|u_2|_{r,\tau} + C\tau^{r-\frac{3}{2}}N^{\frac{7}{2}-r}|u_1|_{r,\tau}\\ &= C\tau^{r-\frac{3}{2}}N^{\frac{7}{2}-r}\left(|u_1|_{r,\tau}+|u_2|_{r,\tau}\right).\end{aligned} \tag{2.79}$$

Using (2.79) and (2.68) with $m=2$, we obtain

$$\begin{aligned}\|\partial_t E_2^N\|_\tau &\le \|\partial_t E_2^N(t) - \partial_t E_2^N(0)\|_\tau + \|\partial_t E_2^N(0)\|_\tau\\ &= \|\partial_t E_2^N(t) - \partial_t E_2^N(0)\|_\tau + \tau^{\frac{1}{2}}|\partial_t E_2^N(0)|\\ &\le C\tau\Big(\|\partial_t E_2^N\|_\tau + \|E_2^N\|_\tau + \tau^{r-2}N^{\frac{7}{2}-r}\left(|u_1|_{r,\tau}+|u_2|_{r,\tau}\right)\Big).\end{aligned} \tag{2.80}$$

Then (2.80) can be rewritten as

$$\|\partial_t E_2^N\|_\tau \le C\tau\|E_2^N\|_\tau + C\tau^{r-1}N^{\frac{7}{2}-r}\left(|u_1|_{r,\tau}+|u_2|_{r,\tau}\right) \tag{2.81}$$

for sufficiently small τ. Similar to the derivation of (2.58), we deduce that

$$\|E_2^N\|_\tau \le \sqrt{2}\tau^{\frac{1}{2}}|E_2^N(0)| + 2\tau\|\partial_t E_2^N\|_\tau. \tag{2.82}$$

Inserting (2.78) and (2.81) into (2.82) yields

$$\|E_2^N\|_\tau \le C\tau^2\|E_2^N\|_\tau + C\tau^r N^{\frac{7}{2}-r}\left(|u_1|_{r,\tau}+|u_2|_{r,\tau}\right),$$

which implies that

$$\|E_2^N\|_T \le C\tau^r N^{\frac{7}{2}-r}\left(|u_1|_{r,\tau}+|u_2|_{r,\tau}\right) \tag{2.83}$$

for sufficiently small τ. Inserting (2.83) into (2.81) gives

$$\|\partial_t E_2^N\|_\tau \le C\tau^{r-1}N^{\frac{7}{2}-r}\left(|u_1|_{r,\tau}+|u_2|_{r,\tau}\right). \tag{2.84}$$

Moreover, inserting (2.83) and (2.84) into (2.84), leads to

$$|\partial_t E_2^N(\tau) - \partial_t E_2^N(0)| \le C\tau^{r-\frac{3}{2}}N^{\frac{7}{2}-r}\left(|u_1|_{r,\tau}+|u_2|_{r,\tau}\right),$$

which together with (2.79) yields

$$\begin{aligned}|\partial_t E_2^N(\tau)| &\le |\partial_t E_2^N(\tau) - \partial_t E_2^N(0)| + |\partial_t E_2^N(0)|\\ &\le C\tau^{r-\frac{3}{2}}N^{\frac{7}{2}-r}\left(|u_1|_{r,\tau}+|u_2|_{r,\tau}\right).\end{aligned} \tag{2.85}$$

Combining (2.13) and (2.83), we obtain

$$\|u_2 - u_2^N\|_\tau \le \|u_2 - \mathcal{I}_{\tau,N}u_2\|_\tau + \|E_2^N\|_\tau \le C\tau^r N^{\frac{7}{2}-r}\left(|u_1|_{r,\tau}+|u_2|_{r,\tau}\right).$$

Similarly, combining (2.14) and (2.84), we get

$$\|\partial_t u_2 - \partial_t u_2^N\|_\tau \le \|\partial_t(u_2 - \mathcal{I}_{\tau,N}u_2)\|_\tau + \|\partial_t E_2^N\|_\tau \le C\tau^{r-1}N^{\frac{7}{2}-r}\left(|u_1|_{r,\tau}+|u_2|_{r,\tau}\right).$$

Noting the fact that $u_2(\tau)=\mathcal{I}_{\tau,N}u_2(\tau)$, then using (2.52), (2.61) and (2.62), we find

$$\begin{aligned}|u_2(\tau)-u_2^N(\tau)| &= |E_2^N(\tau)| \le \tau^{-\frac12}\|E_2^N\|_\tau + \tau^{\frac12}\|\partial_t E_2^N\|_\tau \\ &\le C\tau^{r-\frac12}N^{\frac72-r}\left(|u_1|_{r,\tau}+|u_2|_{r,\tau}\right).\end{aligned}$$

Combining (2.14) and (2.85), we deduce that

$$\begin{aligned}|\partial_t u_2(\tau)-\partial_t u_2^N(\tau)| &\le |\partial_t u_2(\tau)-\partial_t\mathcal{I}_{\tau,N}u_2(\tau)| + |\partial_t E_2^N(\tau)| \\ &\le C\tau^{r-\frac32}N^{\frac72-r}\left(|u_1|_{r,\tau}+|u_2|_{r,\tau}\right).\end{aligned}$$

Repeating the above process, we conclude that for $1\le m\le M$, there hold

$$\|u_m-u_m^N\|_\tau \le C\tau^r N^{\frac72-r}\sum_{j=1}^m |u_j|_{r,\tau}, \tag{2.86}$$

$$\|\partial_t u_m-\partial_t u_m^N\|_\tau \le C\tau^{r-1}N^{\frac72-r}\sum_{j=1}^m |u_j|_{r,\tau}, \tag{2.87}$$

$$|u_m(\tau)-u_m^N(\tau)| \le C\tau^{r-\frac12}N^{\frac72-r}\sum_{j=1}^m |u_j|_{r,\tau}, \tag{2.88}$$

$$|\partial_t u_m(\tau)-\partial_t u_m^N(\tau)| \le C\tau^{r-\frac32}N^{\frac72-r}\sum_{j=1}^m |u_j|_{r,\tau}. \tag{2.89}$$

Consequently, using (2.86) and the Cauchy-Schwarz inequality gives

$$\begin{aligned}\|u-u^N\|_{L^2(0,m\tau)} &= \left(\sum_{k=1}^m \|u_k-u_k^N\|_\tau^2\right)^{\frac12} \le C\tau^r N^{\frac72-r}\left(\sum_{k=1}^m k|u|^2_{H^r(0,k\tau)}\right)^{\frac12} \\ &\le Cm\tau^r N^{\frac72-r}|u|_{H^r(0,m\tau)},\end{aligned}$$

which implies (2.70). Similarly, using (2.87) and the Cauchy-Schwarz inequality gives

$$\begin{aligned}\|\partial_t u-\partial_t u^N\|^2_{L^2(0,m\tau)} &= \left(\sum_{k=1}^m \|\partial_t u_k-\partial_t u_k^N\|_\tau^2\right)^{\frac12} \le C\tau^{2(r-1)}N^{7-2r}\left(\sum_{k=1}^m k|u|^2_{H^r(0,k\tau)}\right)^{\frac12} \\ &\le Cm\tau^{r-1}N^{\frac72-r}|u|_{H^r(0,m\tau)},\end{aligned}$$

which implies (2.71). Moreover, using (2.88), (2.89) and the Cauchy-Schwarz inequality yields

$$\begin{aligned}&|u(m\tau)-u^N(m\tau)| = |u_m(\tau)-u_m^N(\tau)| \le Cm^{\frac12}\tau^{r-\frac12}N^{\frac72-r}|u|_{H^r(0,m\tau)}, \\ &|\partial_t u(m\tau)-\partial_t u^N(m\tau)| = |\partial_t u_m(\tau)-\partial_t u_m^N(\tau)| \le Cm^{\frac12}\tau^{r-\frac32}N^{\frac72-r}|u|_{H^r(0,m\tau)}.\end{aligned}$$

This proves (2.72) and (2.73). □

Remark 2.4. If $\partial_r u\in L^\infty(0,T)$, then the error estimates in Theorem 2.2 imply that

$$\begin{aligned}&\|u-u^N\|_{L^2(0,T)} = \mathcal{O}(\tau^{r-\frac12}N^{\frac72-r}), \quad \|\partial_t u-\partial_t u^N\|_{L^2(0,T)} = \mathcal{O}(\tau^{r-\frac32}N^{\frac72-r}), \\ &|u(T)-u^N(T)| = \mathcal{O}(\tau^{r-1}N^{\frac72-r}), \quad |\partial_t u(T)-\partial_t u^N(T)| = \mathcal{O}(\tau^{r-2}N^{\frac72-r}).\end{aligned}$$

Thus, the multi-interval LGR collocation scheme converges either as the step-size τ is decreased or as N is increased.

The multi-interval LGR collocation scheme can also be applied to system of second-order ODEs of the form

$$\begin{cases} \partial_t^2 \vec{u}(t) = \vec{f}(\partial_t \vec{u}(t), \vec{u}(t), t), & 0 < t \le T, \\ \partial_t \vec{u}(0) = \vec{v}_0, \quad \vec{u}(0) = \vec{u}_0, \end{cases} \tag{2.90}$$

where

$$\vec{u}(t) = \left(u^1(t), u^2(t), \cdots, u^n(t)\right)^T,$$
$$\vec{f}(\partial_t \vec{u}(t), \vec{u}(t), t) = \left(f^1(\partial_t \vec{u}(t), \vec{u}(t), t), f^2(\partial_t \vec{u}(t), \vec{u}(t), t), \cdots, f^n(\partial_t \vec{u}(t), \vec{u}(t), t)\right)^T$$

are vector valued functions, $\vec{v}_0$ and $\vec{u}_0$ are given vectors.

Then, the multi-interval LGR collocation scheme for (2.90) can be read as: Find $\vec{u}_m^{N_m}(t) \in (\mathcal{P}_{N_m+2}(0, \tau_m))^n$ such that

$$\begin{cases} \partial_t^2 \vec{u}_m^{N_m}(t_{\tau_m,k}^{N_m}) = f(\partial_t \vec{u}_m^{N_m}(t_{\tau_m,k}^{N_m}), \vec{u}_m^{N_m}(t_{\tau_m,k}^{N_m}), T_{m-1} + t_{\tau_m,k}^{N_m}), & 0 \le k \le N_m, \quad 1 \le m \le M, \\ \partial_t \vec{u}_m^{N_m}(0) = \partial_t \vec{u}_{m-1}^{N_{m-1}}(\tau_{m-1}), \quad \vec{u}_m^{N_m}(0) = \vec{u}_{m-1}^{N_{m-1}}(\tau_{m-1}), & 2 \le m \le M, \\ \partial_t \vec{u}_1^{N_1}(0) = \vec{v}_0, \quad \vec{u}_1^{N_1}(0) = \vec{u}_0. \end{cases} \tag{2.91}$$

Clearly, the global numerical solution $\vec{u}^N(t)$ of (2.90) is given by

$$\vec{u}^N(T_{m-1} + t) = \vec{u}_m^{N_m}(t), \quad 0 \le t \le \tau_m, \quad 1 \le m \le M. \tag{2.92}$$

2.5. Numerical examples

In this section, we present some numerical examples to illustrate the performance of the single and multi-interval LGR collocation methods.

2.5.1. Oscillating solution

Consider the linear problem ([33])

$$\begin{cases} u''(t) = -\omega^2 u(t) + (\omega^2 - 1)\sin t, & 0 < t \le T, \\ u'(0) = \omega + 1, \quad u(0) = 1 \end{cases} \tag{2.93}$$

with oscillating solution given by $u(t) = \cos \omega t + \sin \omega t + \sin t$.

We first consider the performance of the single-interval LGR collocation scheme (2.21) for problem (2.93) with $T = 1$ and different ω. In Figs. 2.1 and 2.2, we plot the absolute function value error $E^N(T) := |u(T) - u^N(T)|$ and derivative error $\partial_t E^N(T) := |\partial_t u(T) - \partial_t u^N(T)|$ against N in a semi-log scale, respectively. It can be seen that the numerical errors decay exponentially as N increases.

We next test the multi-interval LGR collocation scheme (2.65) (with uniform step-size $\tau_m \equiv \tau$) for problem (2.93) with $T = 100$ and different ω. In Figs. 2.3 and 2.4, we plot the absolute errors $E^N(T)$ and $\partial_t E^N(T)$ of the multi-interval scheme (2.65) with $N = 12$ and different τ. Clearly, the multi-interval LGR collocation scheme is stable and accurate for large T.

Finally, we compare our method with some commonly used numerical methods for solving oscillatory problems. To this end, we denote these methods as follows:

- ARKN: The six-stage adapted Runge-Kutta-Nyström method of fifth-order developed by Franco [14].

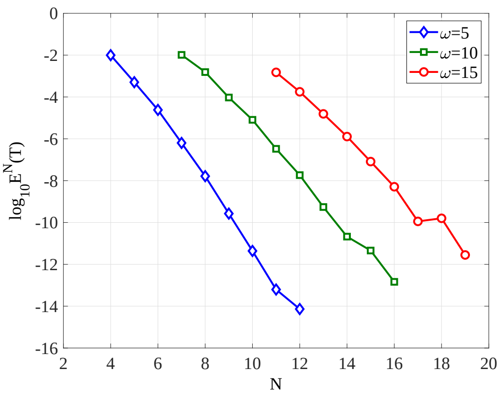

Fig. 2.1. Function value error: single-interval scheme (2.21) for problem (2.93).

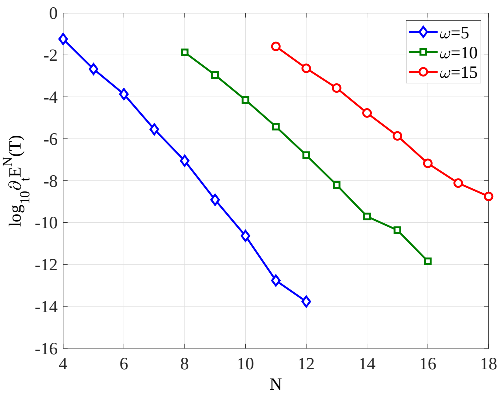

Fig. 2.2. Derivative error: single-interval scheme (2.21) for problem (2.93).

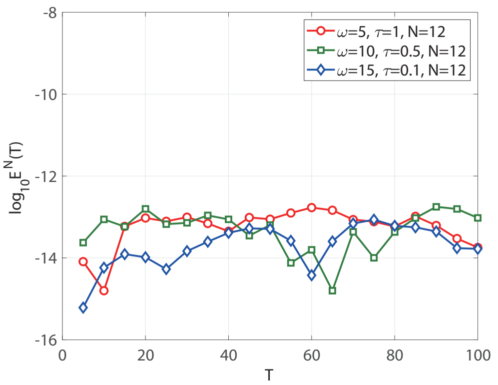

Fig. 2.3. Function value error: multi-interval scheme (2.65) for problem (2.93).

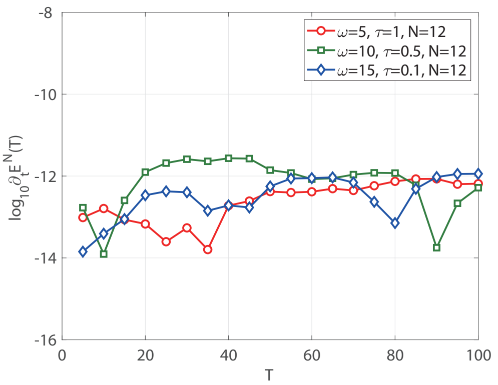

Fig. 2.4. Derivative error: multi-interval scheme (2.65) for problem (2.93).

- Trig-1: The trigonometric fitted integrator developed by Gautschi [17].
- Trig-2: The trigonometric fitted integrator developed by Deuflhard [12].
- Trig-3: The trigonometric fitted integrator developed by Hairer and Lubich [27].
- MLGRC: The multi-interval LGR collocation method proposed in this paper.

We solve the problem (2.93) with $T = 100$ and different ω, by using the ARKN method and MLGRC method with $N = 5$, respectively. In Table 2.1, we list the CPU elapsed times (CPUT) and errors $E^N(T)$ for different ω and step-size τ. It can be seen that although the MLGRC method requires more CPU time, it provides much more accurate results than the ARKN method.

We also make a simple comparison between the Trig-1, Trig-2, Trig-3 methods (see the methods (A), (B) and (E) in Section XIII.2.2 of [28]) and the MLGRC method (with $N = 1$ and 2) for solving the problem (2.93) with $T = 10$. In Figs. 2.5 and 2.6, we plot the errors $E^N(T)$ against $1/\tau$ in a log-log scale for $\omega = 5$ and 15, respectively. Here, τ is the uniform time step-size. It can be seen that the MLGRC method exhibits higher convergence orders and provides much more accurate results than the Trig-1, Trig-2, and Trig-3 methods.

Table 2.1: Numerical comparison of the ARKN and MLGRC methods for problem (2.93).

ω	τ	ARKN		MLGRC	
		CPUT	$E^N(T)$	CPUT	$E^N(T)$
5	0.05	0.0258	1.0968 E-06	0.1967	1.0769 E-13
	0.10	0.0252	3.7403 E-05	0.1126	1.6475 E-13
	0.25	0.0169	4.3402 E-03	0.0652	5.0199 E-09
10	0.025	0.0444	5.7196 E-07	0.3407	1.1413 E-13
	0.05	0.0275	2.0454 E-05	0.2460	3.9435 E-13
	0.10	0.0239	8.5573 E-04	0.1222	8.7454 E-10
15	0.025	0.0429	3.3092 E-06	0.3639	8.1934 E-14
	0.05	0.0258	1.4367 E-04	0.2544	4.3870 E-11
	0.10	0.0241	7.4586 E-03	0.1487	8.3910 E-08

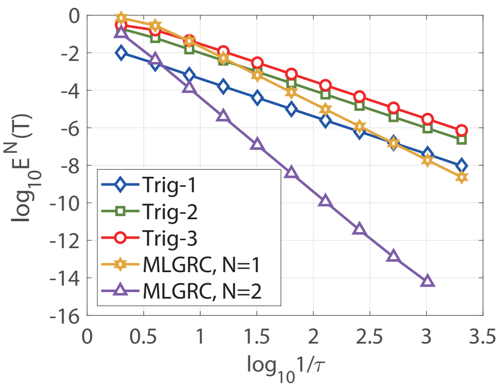

Fig. 2.5. Comparison of different methods for problem (2.93) with $T = 10$ and $\omega = 5$.

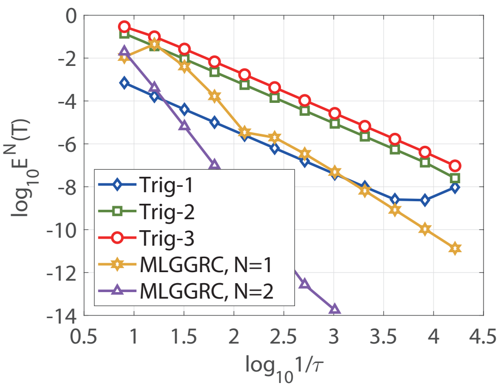

Fig. 2.6. Comparison of different methods for problem (2.93) with $T = 10$ and $\omega = 15$.

2.5.2. Hamilton system

Consider the two-body problem ([50])

$$\begin{cases} q_1''(t) = -\dfrac{q_1(t)}{(q_1^2(t)+q_2^2(t))^{3/2}}, & 0 < t \le T, \\ q_2''(t) = -\dfrac{q_2(t)}{(q_1^2(t)+q_2^2(t))^{3/2}}, & 0 < t \le T, \\ q_1(0) = 1-e, \quad q_1'(0) = 0, \\ q_2(0) = 0, \quad q_2'(0) = \sqrt{\dfrac{1+e}{1-e}}, \end{cases} \tag{2.94}$$

where $e \in [0, 1)$ is the eccentricity of elliptical orbit. It is well-known that the Hamiltonian function of the system is defined as

$$H(t) := \frac{1}{2}\left(p_1^2(t) + p_2^2(t)\right) - \frac{1}{(q_1^2(t)+q_2^2(t))^{\frac{1}{2}}},$$

where $p_1(t) = q_1'(t)$ and $p_2(t) = q_2'(t)$.

For description of the numerical errors, we denote by $q_1^N(t)$ and $q_2^N(t)$ the LGR collocation approximations to $q_1(t)$ and $q_2(t)$, respectively. We further denote by $H^N(t)$ the numerical energy of the Hamiltonian, and by $E^N(t)$ the energy error at t, namely,

$$E^N(t) = |H^N(t) - H(0)|. \tag{2.95}$$

Here, $H(0)$ is the initial energy of the Hamiltonian.

We first consider the performance of the multi-interval LGR collocation scheme (2.91) with uniform step-size $\tau = 1$ and uniform mode $N = 15$ for problem (2.94) with $e = 0.2$. In Fig. 2.7, we plot the point-wise energy errors $E^N(t)$ for $t \in [0, 10^7]$. It can be seen that the multi-interval scheme (2.91) is stable and accurate for long-time computation. In Fig. 2.8, we also plot the numerical orbit $(q_1^N(t), q_2^N(t))$ for $t \in [0, 10^7]$. Clearly, the long-time behaviour of the numerical orbit is highly stable.

We next compare the multi-interval LGR collocation (MLGRC) method (2.91) with some existing numerical methods for solving the problem (2.94). For simplicity, we denote these methods as follows:

- TSHM: The eighth-order standard two-step hybrid method derived by Tsitouras [46].
- EFMTSH: The eighth-order exponentially fitted modified two-step hybrid method with seven-stage derived by Franco and Rández [15].
- MLGC-1: The multi-interval Legendre-Gauss collocation method with Newton-Raphson iteration developed by Guo and Yan [24].
- MLGC-2: The multi-interval Legendre-Gauss collocation method with simple fixed-point iteration developed by Yi and Wang [54].

We solve the problem (2.94) with $e = 0.2$, by using the TSHM method, EFMTSH method and MLGRC method with $N = 8$, respectively. In Table 2.2, we list the CPU elapsed times and energy errors $E^N(t)$ at different time t. It can be seen that although our method requires more CPU time at each time step, it provides much more accurate results than the TSHM and EFMTSH methods. In particular, the MLGRC method is valid for large step-size τ. However,

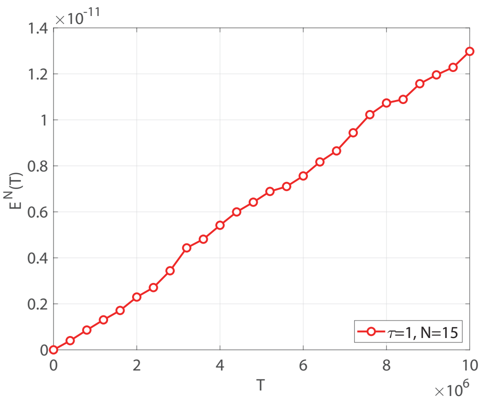

Fig. 2.7. Multi-interval scheme (2.91) for problem (2.94) with $\tau = 1$ and $N = 15$.

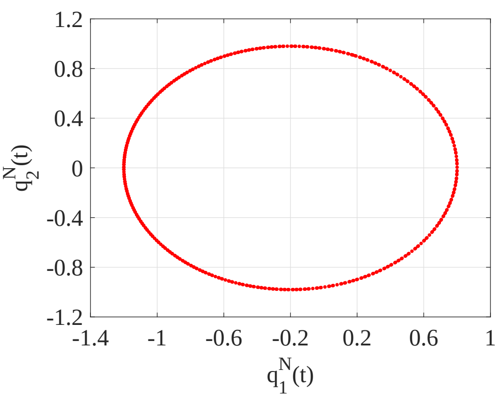

Fig. 2.8. Numerical orbit $(q_1^N(t), q_2^N(t))$ of problem (2.94) for $0 \le t \le 10^7$.

Table 2.2: Comparison of different numerical methods for problem (2.94).

τ	t	TSHM		EFMTSH		MLGRC	
		CPUT	$E^N(t)$	CPUT	$E^N(t)$	CPUT	$E^N(t)$
0.25	1000	0.1118	6.4189 E-03	0.1044	1.4908 E-03	1.2742	8.8818 E-15
	1500	0.1669	1.4453 E-02	0.1270	3.3536 E-03	1.8976	1.1435 E-14
	2000	0.2135	2.5703 E-02	0.1714	5.9612 E-03	2.5593	1.1102 E-14
0.5	1500	0.0879	4.2660 E-01	0.0833	1.5620 E-00	0.9612	1.3323 E-14
	2000	0.0993	7.3980 E-01	0.1206	1.9970 E-00	1.2499	1.0103 E-14
	2500	0.1468	5.7285 E-01	0.1258	1.1844 E-00	1.5728	1.5876 E-14
1	2000	0.0531	2.2719 E-00	0.0637	7.8570 E+03	0.6479	1.4834 E-10
	2500	0.0811	1.4269 E-00	0.0994	9.9634 E+03	0.8254	1.8521 E-10
	3000	0.0826	1.6254 E-00	0.0764	1.2073 E+04	0.9835	2.2212 E-10

Table 2.3: Comparison of different spectral collocation methods for problem (2.94).

t	MLGC-1		MLGC-2		MLGRC	
	CPUT	$E^N(t)$	CPUT	$E^N(t)$	CPUT	$E^N(t)$
2000	4.6666	5.8842 E-15	2.0419	1.3212 E-14	2.0010	5.6066 E-15
4000	9.0601	3.5638 E-14	3.8171	1.5321 E-14	3.8759	5.2736 E-15
8000	17.9995	7.4274 E-14	7.8588	3.4417 E-15	7.9151	1.7653 E-14
16000	35.8767	1.4355 E-13	16.8501	6.4226 E-14	15.9260	3.6637 E-15
32000	72.0180	2.2515 E-13	31.5332	6.8612 E-14	31.9837	1.5321 E-14
64000	143.8829	4.5464 E-13	64.4375	1.2845 E-13	64.3382	7.3941 E-14

this is not the case for the other two methods. Hence, we can save the total computational time if we use bigger time step-size.

We also compare the performances of the MLGRC, MLGC-1 and MLGC-2 methods for solving the problem (2.94) with $e = 0.2$. For these three methods, we use uniform step-size $\tau = 1$ and uniform mode $N = 14$. In Table 2.3, we list the CPU elapsed times and energy errors $E^N(t)$ at different time t. It can be observed that although the three methods show high accuracy, the MLGRC and MLGC-2 methods require much less CPU time than the MLGC-1 method.

2.5.3. Singular solution

Consider the nonlinear problem

$$\begin{cases} u''(t) = \sin(u'(t)) + \cos(u(t)) + g(t), \quad 0 < t \leq T, \\ u'(0) = 0, \quad u(0) = 0, \end{cases} \tag{2.96}$$

where $g(t)$ is chosen such that $u(t) = t^r$ with $r > 1$ be a non-integer. Clearly, the solution u has an singularity at $t = 0$.

We first consider the multi-interval LGR collocation scheme (2.65) (with uniform step-size $\tau = 0.1$) for problem (2.96) with $T = 1$. For our purpose, we denote by “Err” the maximum

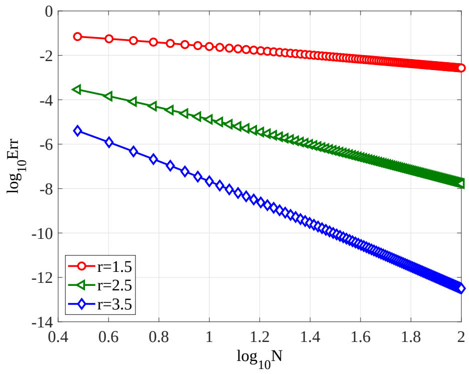

Fig. 2.9. Multi-interval scheme (2.65) for problem (2.96) with uniform step-size $\tau = 0.1$.

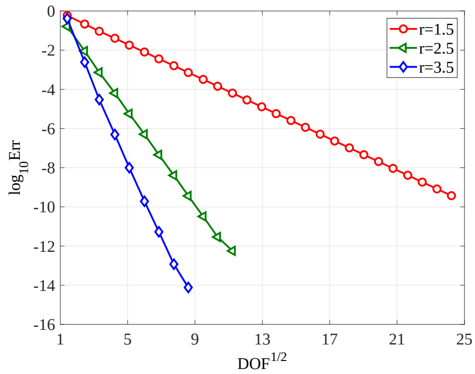

Fig. 2.10. Multi-interval scheme (2.65) for problem (2.96) with geometrically refined time-steps.

nodal error. In Fig. 2.9, we plot the maximum nodal errors against N in a log-log scale for $r = 1.5$, 2.5 and 3.5, respectively. Clearly, we only obtain algebraic convergence rate for each r.

We next consider the multi-interval LGR collocation scheme (2.65) with non-uniform step-sizes and non-uniform approximation degrees. More specifically, we use the concepts of geometrically refined time-steps and linearly increasing approximation degrees from the hp-version Galerkin methods (see, e.g., [39, 49]). To this end, we divide the interval $(0, T]$ into M subintervals $\{I_m := (T_{m-1}, T_m]\}_{m=1}^M$ with nodal points given by

$$T_0 = 0, \quad T_m := T\sigma^{M-m}, \quad 1 \le m \le M,$$

where $\sigma \in (0, 1)$ is called the geometric refinement factor. For each subinterval I_m, we use $N_m + 1$ LGR collocation points with $N_1 = 1$ and $N_m = \max(1, \lfloor \mu m \rfloor)$ for $2 \le m \le M$. Here, $\mu > 0$ and $\lfloor \mu m \rfloor$ denotes the biggest integer smaller than or equal to μm. Let "DOF" be the total number of degrees of freedom. In Fig. 2.10, we plot the maximum nodal errors against the square root of DOF for fixed $\mu = 1.5$ and $\sigma = 0.2$. Clearly, each straight error curve indicates exponential convergence with respect to $\text{DOF}^{1/2}$ for each r.

3. Application to Nonlinear Wave Equations

In this section, we apply the multi-interval LGR spectral collocation method to the simulation of the second-order time dependent PDEs. More specifically, we will adopt the multi-interval LGR spectral collocation method to handle the time integration of the second-order differential system arising after space discretization obtained with the LGL spectral collocation method. Furthermore, we will take two typical nonlinear wave equations as examples to test the high accuracy of the proposed space-time spectral collocation scheme.

3.1. Space-time collocation scheme for second-order evolution equations

Consider the nonlinear second-order evolution equations of the form

$$\begin{cases} \partial_t^2 u = \partial_x^2 u + f(u, \partial_t u, \partial_x u, x, t), & (x,t) \in (-1,1) \times (0,T], \\ u(-1,t) = \alpha(t), \quad u(1,t) = \beta(t), & t \in (0,T], \\ u(x,0) = \varphi(x), \quad \partial_t u(x,0) = \psi(x), & x \in [-1,1] \end{cases} \tag{3.1}$$

with suitable consistent initial and boundary conditions.

Let $\{x_k\}_{k=0}^M$ be the LGL points with $x_0 = -1$ and $x_M = 1$. We denote by $\{\phi_k\}_{k=0}^M$ the corresponding Lagrange basis functions associated with the points $\{x_k\}_{k=0}^M$. Then, the LGL spectral collocation method in space for problem (3.1) is to find $U^M(x,t)$ such that

$$\begin{cases} \partial_t^2 U^M(x_k,t) = \partial_x^2 U^M(x_k,t) + f(U^M(x_k,t), \partial_t U^M(x_k,t), \partial_x U^M(x_k,t), x_k, t), \\ \qquad\qquad\qquad\qquad\qquad\qquad\qquad\qquad 1 \le k \le M-1, \quad t \in (0,T], \\ U^M(-1,t) = \alpha(t), \qquad U^M(1,t) = \beta(t), \qquad\qquad\qquad t \in (0,T], \\ U^M(x_k,0) = \varphi(x_k), \quad \partial_t U^M(x_k,0) = \psi(x_k), \quad 0 \le k \le M. \end{cases} \tag{3.2}$$

Let

$$U^M(x,t) = \sum_{j=0}^{M} u_j(t)\phi_j(x). \tag{3.3}$$

Obviously, there holds $u_k(t) = U^M(x_k,t)$ for $0 \le k \le M$. In particular, we have $u_0(t) = \alpha(t)$ and $u_M(t) = \beta(t)$. Inserting (3.3) into (3.2) results into the following nonlinear second-order differential system:

$$\begin{cases} \partial_t^2 u_k(t) = \sum\limits_{j=0}^{M} u_j(t)\partial_x^2\phi_j(x_k) + f\Big(u_k(t), \partial_t u_k(t), \sum\limits_{j=0}^{M} u_j(t)\partial_x\phi_j(x_k), x_k, t\Big), \\ u_k(0) = \varphi(x_k), \quad \partial_t u_k(0) = \psi(x_k), \qquad 1 \le k \le M-1. \end{cases} \tag{3.4}$$

Then, we can solve the nonlinear second-order differential system (3.4) by using the multi-interval LGR spectral collocation scheme (2.91). Accordingly, we denote by $u_k^N(t)$ the LGR spectral collocation approximation of $u_k(t)$ for $1 \le k \le M-1$. Then, we obtain the fully discrete space-time collocation approximation of problem (3.1), denoted by

$$U^{M,N}(x,t) = \sum_{j=0}^{M} u_j^N(t)\phi_j(x)$$

with $u_0^N(t) = \alpha(t)$ and $u_M^N(t) = \beta(t)$.

3.2. Numerical examples

In this section we present a number of numerical experiments to illustrate the performance of the space-time collocation method for nonlinear wave equations.

For checking the numerical accuracy, we define the numerical error at T by

$$E^{M,N}(T) = \max_{1 \le k \le M-1} |u(x_k,T) - u_k^N(T)|.$$

Here, $\{u_k^N(t)\}_{k=1}^{M-1}$ is the multi-interval LGR collocation approximation (based on $N+1$ collocation points on each time step) of the nonlinear second-order differential system (3.4).

3.2.1. Sine-Gordon equation

Consider the nonlinear sine-Gordon equation

$$\begin{cases} \partial_t^2 u = \partial_x^2 u - \sin u, & (x,t) \in (-1,1) \times (0,T], \\ u(-1,t) = \alpha(t), \quad u(1,t) = \beta(t), & t \in (0,T], \\ u(x,0) = \varphi(x), \quad \partial_t u(x,0) = \psi(x), & x \in [-1,1]. \end{cases} \tag{3.5}$$

We choose suitable initial and boundary conditions such that the exact solution of the problem (3.5) is given by

$$u(x,t) = 4\tan^{-1}(e^{(x-ct)/\sqrt{1-c^2}}) \tag{3.6}$$

and

$$u(x,t) = 4\tan^{-1}(\mathrm{sech}(x)t), \tag{3.7}$$

respectively. Here, c is the velocity of the solitary wave and we take $c = 0.5$ in the following tests.

We first use the space-time collocation method proposed in Section 3.1 to solve problem (3.5) with $T = 1000$ and the exact solutions give by (3.6) and (3.7), respectively. More precisely, we combine the LGL collocation method (with $M+1$ collocation points) in space with the multi-interval LGR collocation method (with uniform N) in time. In Figs. 3.1 and 3.2, we plot the errors $E^{M,N}(T)$ for the space-time collocation method with different M, N and uniform time step-size $\tau = 0.1$. Clearly, the space-time collocation method gives accurate and stable numerical results for both test solutions.

We next consider the convergence rates of the space-time collocation method in space and time, respectively. To this end, we keep the errors in time small by using the multi-interval LGR collocation method with $\tau = 0.1$ and $N = 10$. Fig. 3.3 shows that the numerical errors

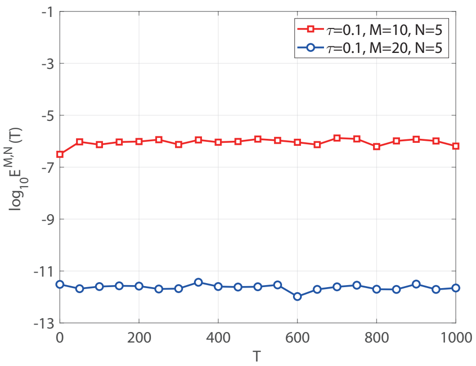

Fig. 3.1. Numerical errors for problem (3.5) with $u(x,t) = 4\tan^{-1}(e^{(x-ct)/\sqrt{1-c^2}})$.

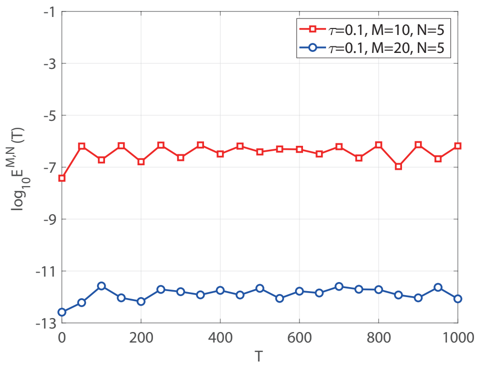

Fig. 3.2. Numerical errors for problem (3.5) with $u(x,t) = 4\tan^{-1}(\mathrm{sech}(x)t)$.

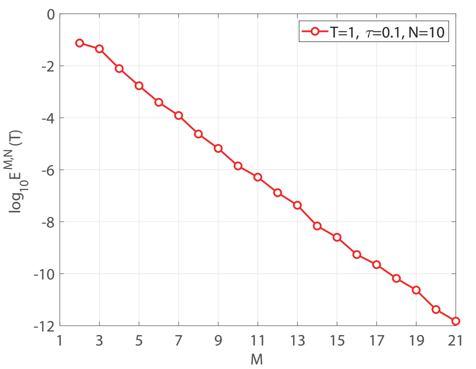

Fig. 3.3. Convergence in space for solution $u(x,t)$ $= 4\tan^{-1}(e^{(x-ct)/\sqrt{1-c^2}})$.

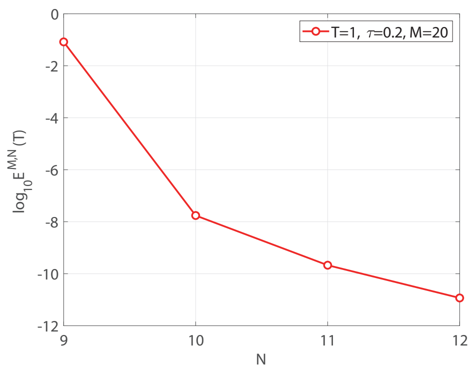

Fig. 3.4. Convergence in time for solution $u(x,t)$ $= 4\tan^{-1}(e^{(x-ct)/\sqrt{1-c^2}})$.

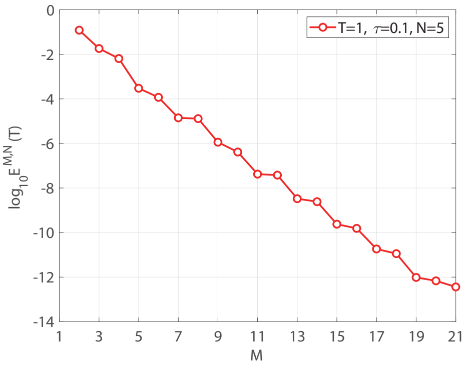

Fig. 3.5. Convergence in space for solution $u(x,t) = 4\tan^{-1}(\text{sech}(x)t)$.

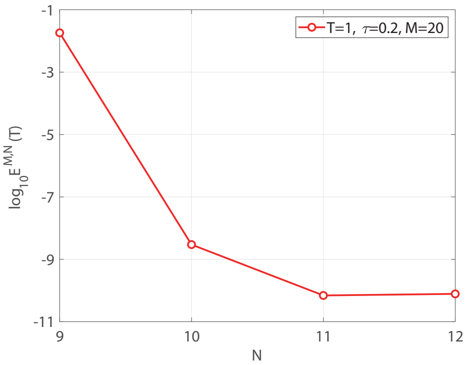

Fig. 3.6. Convergence in time for solution $u(x,t) = 4\tan^{-1}(\text{sech}(x)t)$.

for solution (3.6) decay exponentially as M increases. On the other hand, we keep the errors in space small by using the LGL collocation method with $M = 20$. It can be seen from Fig. 3.4 that the numerical errors for solution (3.6) decay exponentially as N increases. In Figs. 3.5 and 3.6, we plot the numerical errors for solution (3.7). It is clearly to see that the numerical errors decay exponentially both in space and time.

3.2.2. Klein-Gordon equation

Consider the Klein-Gordon equation with quadratic nonlinearity ([37])

$$\begin{cases} \partial_t^2 u = \partial_x^2 u - u^2 - x\cos t + x^2\cos^2 t, & (x,t) \in (-1,1)\times(0,T], \\ u(-1,t) = -\cos t, \quad u(1,t) = \cos t, & t \in (0,T], \\ u(x,0) = x, \qquad \partial_t u(x,0) = 0, & x \in [-1,1]. \end{cases} \tag{3.8}$$

The exact solution is given by $u(x,t) = x\cos t$.

We use the space-time collocation method to solve problem (3.8) with $T = 1000$. In Fig. 3.7, we plot the errors $E^{M,N}(T)$ for the space-time collocation method with different M, N and uniform time step-size $\tau = 0.1$. It can be seen that the space-time collocation method gives

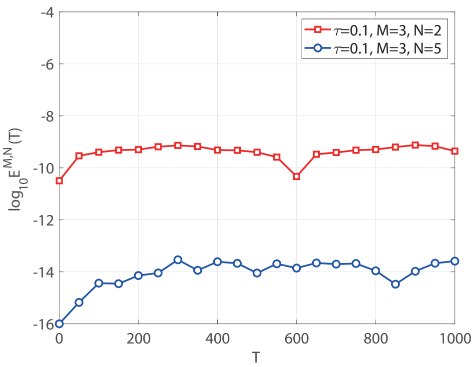

Fig. 3.7. Numerical errors for problem (3.8) with $u(x,t) = x\cos t$.

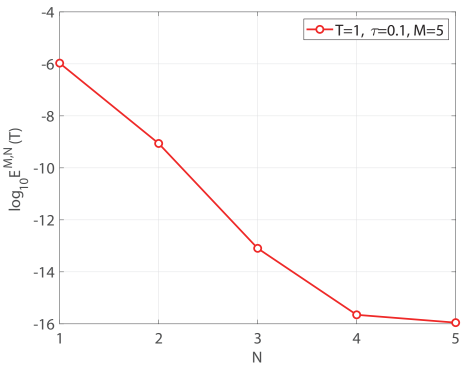

Fig. 3.8. Convergence in time for solution $u(x,t) = x\cos t$.

accurate and stable numerical results again. Since the exact solution is a linear polynomial in space, we only consider the convergence rates of the space-time collocation method in time. Fig. 3.8 shows that the numerical errors decay exponentially as N increases.

We next compare the space-time collocation method presented in Section 3.1 with some existing numerical methods for solving the problem (3.8). For simplicity, we denote these methods as follows:

- RBF: Numerical method based on radial basis functions developed by Dehghan and Shokri [11].
- TSF-1: Numerical method based on tension spline functions developed by Rashidinia and Mohammadi (see method-1 of [37]).
- TSF-2: Numerical method based on tension spline functions developed by Rashidinia and Mohammadi (see method-2 of [37]).
- DQM: Differential quadrature method developed by Pekmen and Tezer-Sezgin [34].
- STSC: Space-time spectral collocation method developed by Yi and Wang [54].

In Table 3.1, we list the L^∞-errors at different time t for different numerical methods. It can be seen that our method and the STSC method with considerably small number of collocation points both in time and space directions (i.e., $\tau = 0.1$, $M = 2$ and $N = 4$) provides much more accurate results than the other methods, which implies that the space-time spectral collocation methods are good choices for numerical solutions of time dependent PDEs with smooth solutions.

Table 3.1: Comparison of different numerical methods for problem (3.8).

t	RBF	TSF-1	TSF-2	DQM	STSC	Present
	L^∞-error	L^∞-error	L^∞-error	L^∞-error	L^∞-error	L^∞-error
1	1.25E-05	1.30E-09	7.68E-10	1.74E-13	1.94E-16	1.66E-16
3	1.56E-05	1.00E-09	7.52E-10	2.68E-12	1.11E-16	2.22E-16
5	3.38E-05	2.56E-10	1.76E-10	3.19E-12	5.00E-16	3.33E-16
7	3.78E-05	1.13E-09	7.63E-10	2.89E-12	4.44E-16	2.22E-16
10	1.31E-05	9.46E-10	6.55E-10	3.60E-12	1.11E-15	6.66E-16

4. Concluding Remarks

In this paper we have presented a single-interval LGR spectral collocation method for nonlinear second-order IVPs of ODEs. We have designed a simple but efficient iterative algorithm based on Legendre polynomial expansion and shown that the single-interval LGR collocation scheme has spectral accuracy. We have also proposed a flexible multi-interval LGR collocation method with variable local time steps and local approximation degrees. A series of numerical experiments show that the multi-interval LGR collocation method exhibits global spectral accuracy and long-time stability. As an application, we have adopted the multi-interval LGR collocation method to handle the time integration of the second-order differential system arising after space discretization of the second-order evolution equation obtained by the LGL collocation method. The numerical simulation results for two typical nonlinear wave equations show that the space-time collocation scheme possesses high accuracy in both space and time. Error analysis of the proposed space-time collocation method for second-order evolution equations will be a topic for our future research.

Acknowledgments. This work is supported in part by the National Natural Science Foundation of China (Grant Nos. 12171322, 11771298 and 11871043), the Natural Science Foundation of Shanghai (Grant Nos. 21ZR1447200, 20ZR1441200 and 22ZR1445500), and the Science and Technology Innovation Plan of Shanghai (Grant No. 20JC1414200).

References

[1] J. An, W.X. Cao, and Z. M. Zhang, An efficient spectral Petrov-Galerkin method for nonlinear Hamiltonian systems, *Commun. Comput. Phys.*, **5**:26 (2019), 1249–1273.

[2] J. An, W. X. Cao, and Z. M. Zhang, A class of efficient spectral methods and error analysis for nonlinear Hamiltonian systems, *Commun. Math. Sci.*, **2**:18 (2020), 395–428.

[3] P. F. Antonietti, I. Mazzieri, N. Dal Santo, and A. Quarteroni, A high-order discontinuous Galerkin approximation to ordinary differential equations with applications to elastodynamics, *IMA J. Numer. Anal.*, **4**:38 (2018), 1709–1734.

[4] I. Babuška and T. Janik, The *h-p* version of the finite element method for parabolic equations: I. The *p*-version in time, *Numer. Methods Partial Differential Equations*, **4**:5 (1989), 363–399.

[5] I. Babuška and T. Janik, The *h-p* version of the finite element method for parabolic equations: II. The *h-p* version in time, *Numer. Methods Partial Differential Equations*, **4**:6 (1990), 343–369.

[6] C. Bernardi and Y. Maday, *Spectral Methods*, in Handbook of Numerical Analysis, Vol. 5, edited by P. G. Ciarlet and J. L. Lions, North-Holland, Amsterdam, 1997.

[7] J.P. Boyd, *Chebyshev and Fourier Spectral Methods*, Second ed., Dover Publications, Inc., Mineola, NY, 2001.

[8] J. C. Butcher, *Numerical Methods for Ordinary Differential Equations*, Second ed., John Wiley & Sons, Ltd., Chichester, 2008.

[9] A. Cangiani, Z.N. Dong, and E.H. Georgoulis, *hp*-version space-time discontinuous Galerkin methods for parabolic problems on prismatic meshes, *SIAM J. Sci. Comput.*, **4**:39 (2017), A1251–A1279.

[10] C. Canuto, M.Y. Hussaini, A. Quarteroni, and T. A. Zang, *Spectral Methods: Fundamentals in Single Domains*, Springer-Verlag, Berlin, 2006.

[11] M. Dehghan and A. Shokri, Numerical solution of the nonlinear Klein-Gordon equation using radial basis functions, *J. Comput. Appl. Math.*, **2**:230 (2009), 400–410.

[12] P. Deuflhard, A study of extrapolation methods based on multistep schemes without parasitic solutions, *Z. Angew. Math. Phys.*, **2**:30 (1979), 177–189.

[13] D. Devaud, Petrov-Galerkin space-time *hp*-approximation of parabolic equations in $H^{1/2}$, *IMA J. Numer. Anal.*, **4**:40 (2020), 2717–2745.

[14] J.M. Franco, Runge-Kutta-Nyström method adapted to the numerical integration of perturbed oscillators, *Comput. Phys. Comm.*, **3**:147 (2002), 770–787.

[15] J.M. Franco and L. Rández, A class of explicit high-order exponentially-fitted two-step methods for solving oscillatory IVPs, *J. Comput. Appl. Math.*, **342** (2018), 210–224.

[16] D. Funaro, *Polynomial Approximations of Differential Equations*, Springer-Verlag, Berlin, 1992.

[17] W. Gautschi, Numerical integration of ordinary differential equations based on trigonometric polynomials, *Numer. Math.*, **3** (1961), 381-397.

[18] D. Gottlieb and S.A. Orszag, *Numerical Analysis of Spectral Methods: Theory and Applications*, SIAM-CBMS, Philadelphia, 1977.

[19] B. Y. Guo, *Spectral Methods and Their Applications*, World Scientific Publishing Co., Inc., River Edge, NJ, 1998.

[20] B.Y. Guo and Z.Q. Wang, Numerical integration based on Laguerre-Gauss interpolation, *Comput. Methods Appl. Mech. Engrg.*, **37-40**:196 (2007), 3726–3741.

[21] B.Y. Guo and Z.Q. Wang, Legendre-Gauss collocation methods for ordinary differential equations, *Adv. Comput. Math.*, **3**:30 (2009), 249–280.

[22] B.Y. Guo and Z.Q. Wang, A spectral collocation method for solving initial value problems of first order ordinary differential equations, *Discrete Contin. Dyn. Syst. Ser. B*, **3**:14 (2010), 1029–1054.

[23] B.Y. Guo, Z.Q. Wang, H.J. Tian, and L.L. Wang, Integration processes of ordinary differential equations based on Laguerre-Radau interpolations, *Math. Comp.*, **261**:77 (2008), 181–199.

[24] B. Y. Guo and J.P. Yan, Legendre-Gauss collocation methods for initial value problems of second order ordinary differential equations, *Appl. Numer. Math.*, **6**:59 (2009), 1386–1408.

[25] E. Hairer, S.P. Nørsett, and G. Wanner, *Solving Ordinary Differential Equation I: Nonstiff Problems*, Springer-Verlag, Berlin, 1987.

[26] E. Hairer and G. Wanner, *Solving Ordinary Differential Equation II: Stiff and Differential–Algebraic Problems*, Springer-Verlag, Berlin, 1991.

[27] E. Hairer and C. Lubich, Long-time energy conservation of numerical methods for oscillatory differential equations, *SIAM J. Numer. Anal.*, **2**:38 (2000), 414–441.

[28] E. Hairer, C. Lubich, and G. Wanner, *Geometric Numerical Integration: Structure-Preserving Algorithms*, Springer Series in Computational Mathematics, Vol. 31, Springer-Verlag, Berlin, 2006.

[29] J.D. Lambert, *Numerical Methods for Ordinary Differential Systems: The Initial Value Problem*, John Wiley & Sons, Ltd., Chichester, 1991.

[30] S.H. Lui, Legendre spectral collocation in space and time for PDEs, *Numer. Math.*, **1**:136 (2017), 75–99.

[31] S.H. Lui and S. Nataj, Spectral collocation in space and time for linear PDEs, *J. Comput. Phys.*, **424** (2021), Paper No. 109843, 22 pp.

[32] K. Mustapha, H. Brunner, H. Mustapha, and D. Schötzau, An *hp*-version discontinuous Galerkin method for integro-differential equations of parabolic type, *SIAM J. Numer. Anal.*, **4**:49 (2011) 1369–1396.

[33] B. Paternoster, Runge-Kutta(-Nyström) methods for ODEs with periodic solutions based on trigonometric polynomials, *Appl. Numer. Math.*, **2-4**:28 (1998), 401–412.

[34] B. Pekmen and M. Tezer-Sezgin, Differential quadrature solution of nonlinear Klein-Gordon and sine-Gordon equations, *Comput. Phys. Commun.*, **8**:183 (2012), 1702–1713.

[35] Y.H. Qin and H.P. Ma, Legendre-tau-Galerkin and spectral collocation method for nonlinear evolution equations, *Appl. Numer. Math.*, **153** (2020), 52–65.

[36] A. Quarteroni, R. Sacco, and F. Saleri, *Numerical Mathematics*, Second ed., Texts in Applied Mathematics, Vol. 37, Springer-Verlag, Berlin, 2007.

[37] J. Rashidinia and R. Mohammadi, Tension spline approach for the numerical solution of nonlinear Klein-Gordon equation, *Comput. Phys. Comm.*, **1**:181 (2010), 78–91.

[38] D. Schötzau and C. Schwab, Time discretization of parabolic problems by the *hp*-version of the discontinuous Galerkin finite element method, *SIAM J. Numer. Anal.*, **3**:38 (2000), 837–875.

[39] D. Schötzau and C. Schwab, An *hp* a-priori error analysis of the DG time-stepping method for initial value problems, *Calcolo*, **4**:37 (2000), 207–232.

[40] J. Shen, T. Tang, and L.L. Wang, *Spectral Methods: Algorithms, Analysis and Applications*, Springer Series in Computational Mathematics, Vol. 41, Springer, Heidelberg, 2011.

[41] A.M. Stuart and A.R. Humphries, *Dynamical Systems and Numerical Analysis*, Cambridge University Press, Cambridge, 1996.

[42] H. Tal-Ezer, Spectral methods in time for hyperbolic equations, *SIAM J. Numer. Anal.*, **1**:23 (1986), 11–26.

[43] H. Tal-Ezer, Spectral methods in time for parabolic problems, *SIAM J. Numer. Anal.*, **1**:26 (1989), 1–11.

[44] J.G. Tang and H.P. Ma, Single and multi-interval Legendre τ-methods in time for parabolic equations, *Adv. Comput. Math.*, **4**:17 (2002), 349–367.

[45] J.G. Tang and H.P. Ma, A Legendre spectral method in time for first-order hyperbolic equations, *Appl. Numer. Math.*, **1**:57 (2007), 1–11.

[46] Ch. Tsitouras, Explicit eighth order two-step methods with nine stages for integrating oscillatory problems, *Internat. J. Modern Phys. C*, **6**:17 (2006), 861–876.

[47] Z.Q. Wang and B.Y. Guo, Legendre-Gauss-Radau collocation method for solving initial value problems of first order ordinary differential equations, *J. Sci. Comput.*, **1**:52 (2012), 226–255.

[48] Y.C. Wei and L.J. Yi, An *hp*-version of the C^0-continuous Petrov-Galerkin time stepping method for nonlinear second-order initial value problems, *Adv. Comput. Math.*, **4**:46 (2020), Paper No. 56, 25 pp.

[49] T.P. Wihler, An a priori error analysis of the *hp*-version of the continuous Galerkin FEM for nonlinear initial value problems, *J. Sci. Comput.*, **3**:25 (2005), 523–549.

[50] X.Y. Wu, B. Wang, and J.L. Xia, Explicit symplectic multidimensional exponential fitting modified Runge-Kutta-Nyström methods, *BIT Numer. Math.*, **3**:52 (2012), 773–795.

[51] J.P. Yan and B. Y. Guo, Laguerre-Gauss collocation method for initial value problems of second order ODEs, *Appl. Math. Mech.*, **12**:32 (2011), 1541–1564.

[52] J.P. Yan and B.Y. Guo, A collocation method for initial value problems of second-order ODEs by using Laguerre functions, *Numer. Math. Theory Methods Appl.*, **2**:4 (2011), 283–295.

[53] L.J. Yi, An L^∞-error estimate for the *h-p* version continuous Petrov-Galerkin method for nonlinear initial value problems, *East Asian J. Appl. Math.*, **4**:5 (2015), 301–311.

[54] L.J. Yi and Z.Q. Wang, Legendre spectral collocation method for second-order nonlinear ordinary/partial differential equations, *Discrete Contin. Dyn. Syst. Ser. B*, **1**:19 (2014), 299–322.

[55] L.J. Yi and Z.Q. Wang, Legendre-Gauss-type spectral collocation algorithms for nonlinear ordinary/partial differential equations, *Int. J. Comput. Math.*, **7**:91 (2014), 1434–1460.

[56] L.J. Yi and Z.Q. Wang, A Legendre-Gauss-Radau spectral collocation method for first order nonlinear delay differential equations, *Calcolo*, **4**:53 (2016), 691–721.

[57] C. Zhang, H.F. Yao, and H. Y. Li, New space-time spectral and structured spectral element methods for high order problems, *J. Comput. Appl. Math.*, **351** (2019), 153–166.

[58] U. Zrahia and P. Bar-Yoseph, Space-time spectral element method for solution of second-order hyperbolic equations, *Comput. Methods Appl. Mech. Engrg.*, **1-4**:116 (1994), 135–146.